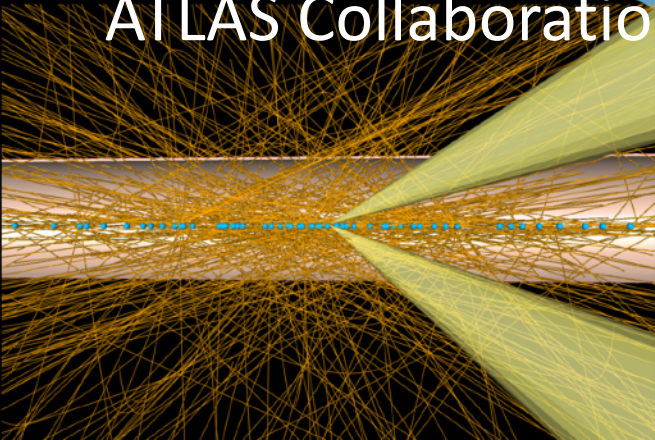




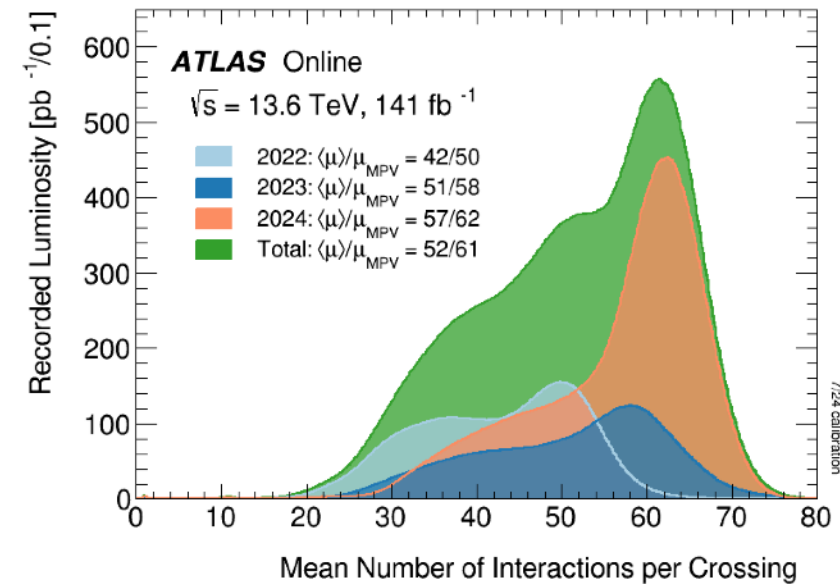
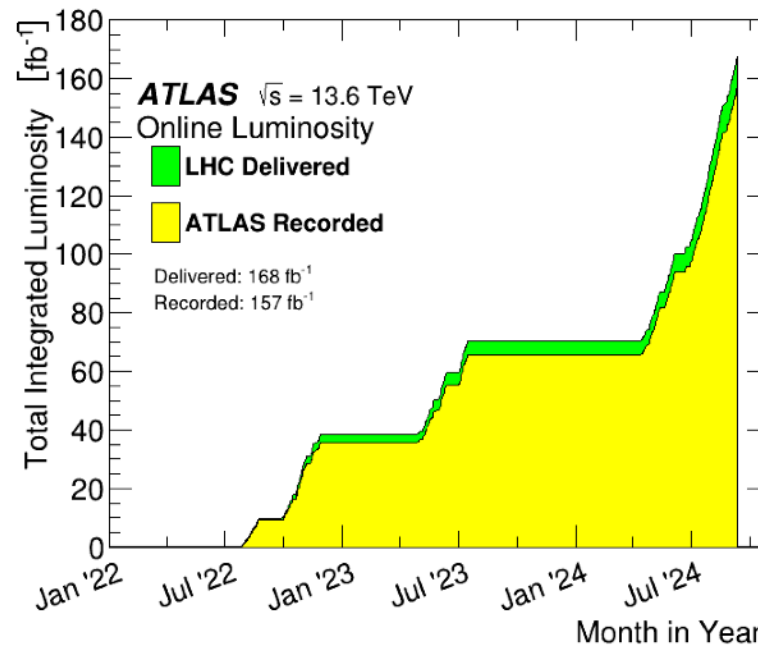
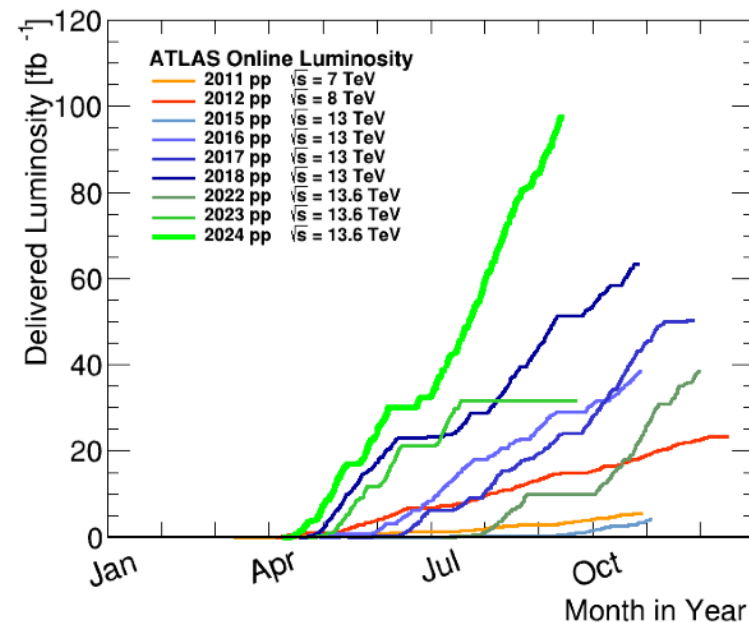
ATLAS Status Report
Antonio De Maria (Nanjing)
on behalf of the
ATLAS Collaboration



Run: 479439
Event: 301428960
2024-07-03 00:11:26 CEST

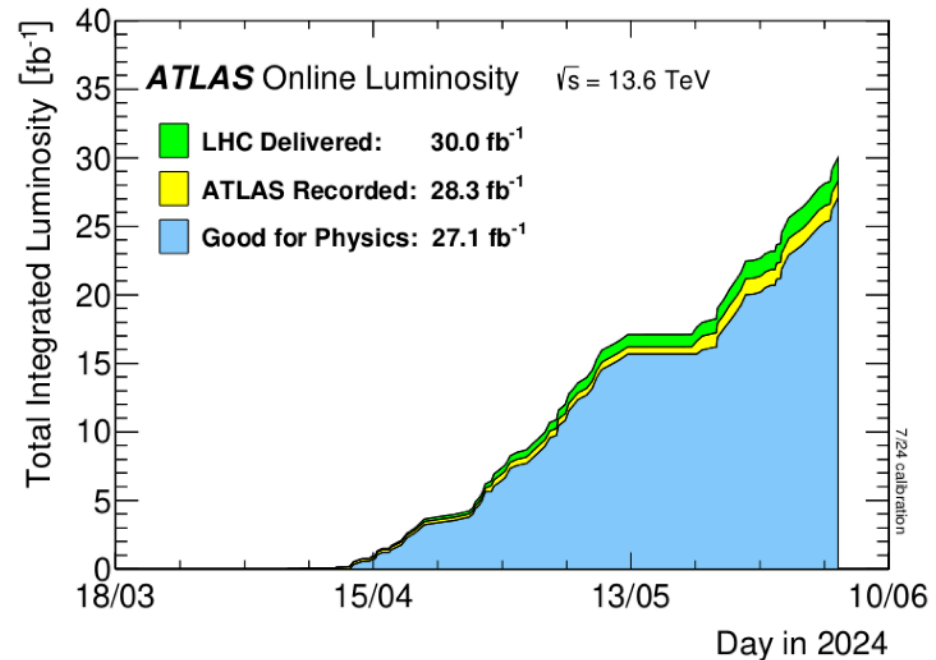
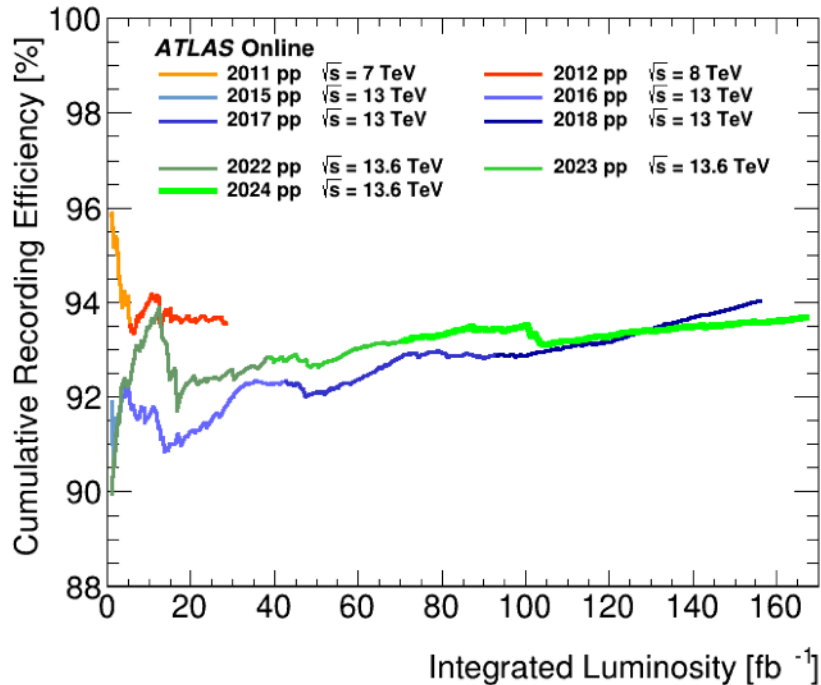
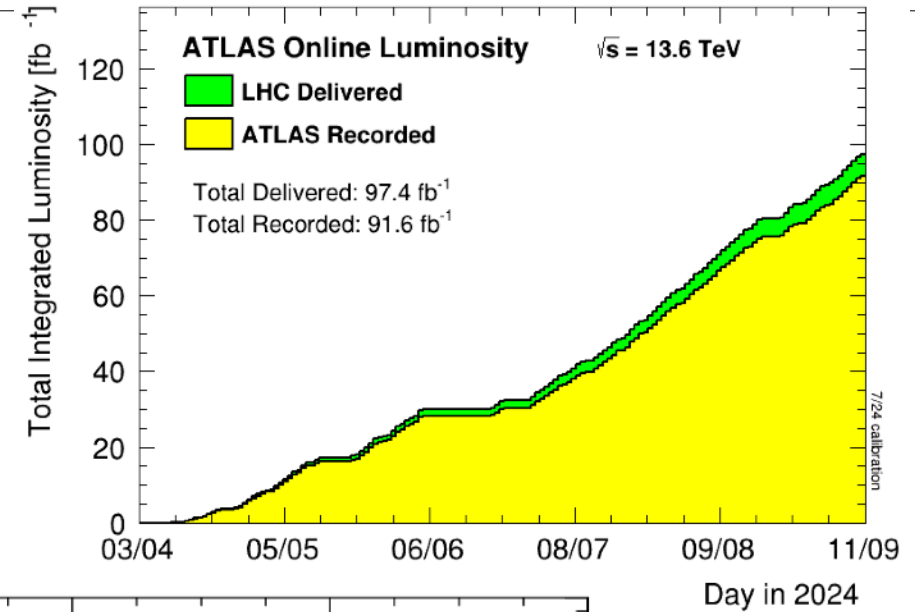
ATLAS operation status for 2024 data taking

- (As of 11 Sep) Collected 91.6 fb^{-1} of data, the most so far in a data-taking year in the shortest amount of time
- In total, collected more data in Run 3 (157 fb^{-1}) with respect to Run 2 (147 fb^{-1})
- Current peak luminosity = $2.15 \cdot 10^{34} \text{ cm}^{-2} \text{ s}^{-1}$, levelling target at $\langle \mu \rangle = 64$:
 - No limitations from High Level Trigger (HLT) CPU, output bandwidth, or readout system
 - No change of thresholds for the single lepton triggers
- Recording efficiency $\sim 94\%$



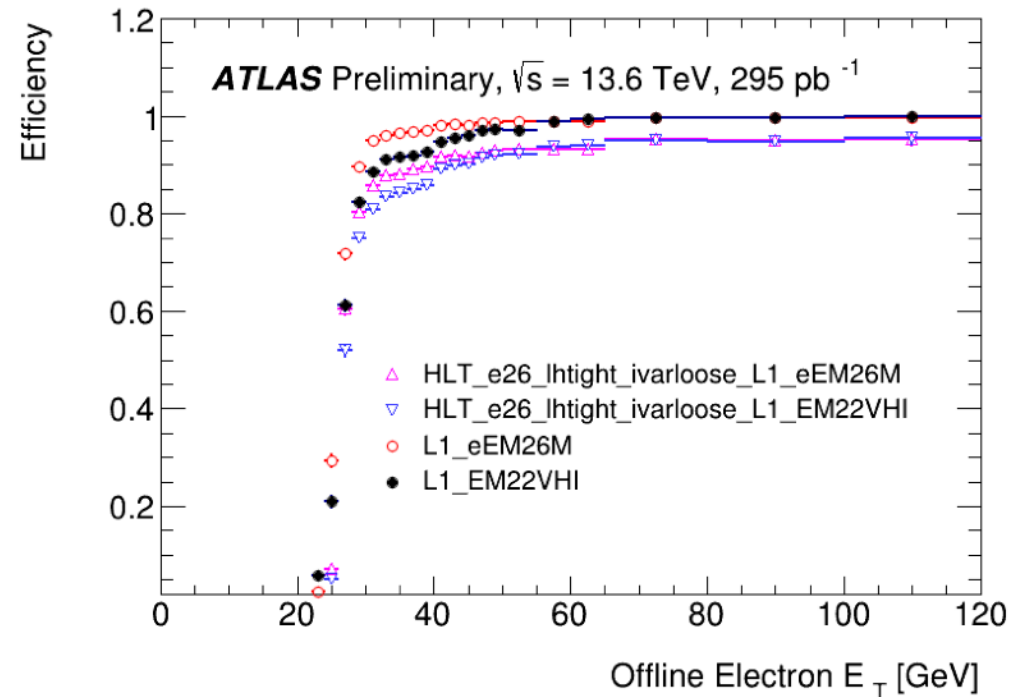
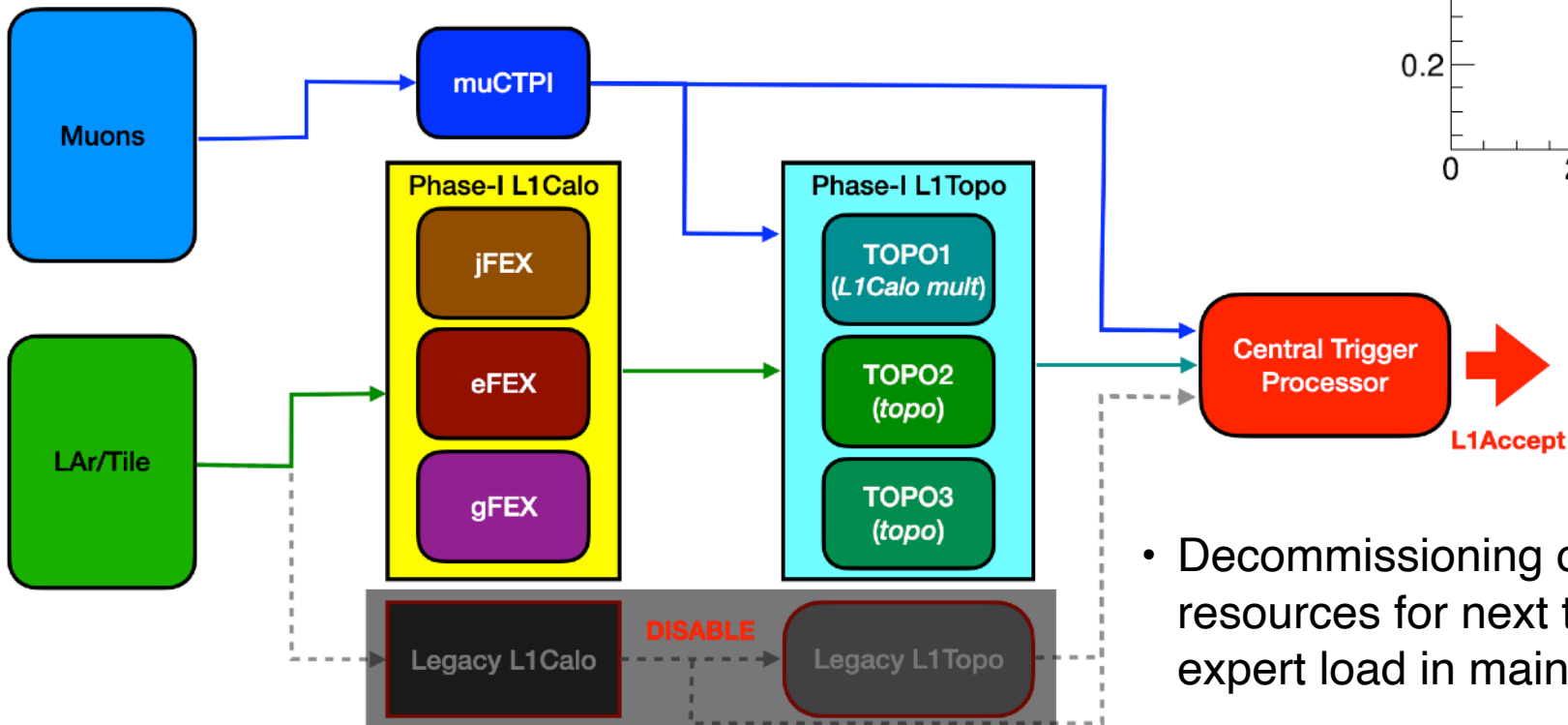
2024 data taking efficiency

- Recording efficiency increases as data-taking continues:
 - Experience and expertise growing in operating the detector
 - Careful follow-up of all issues causing dead-times
 - Continuously improving systems to be more robust against failures/mistakes
- Data Quality assessment completed for data taken until 5th June, with an efficiency $\sim 98\%$



Trigger Level-1 Phase-I update

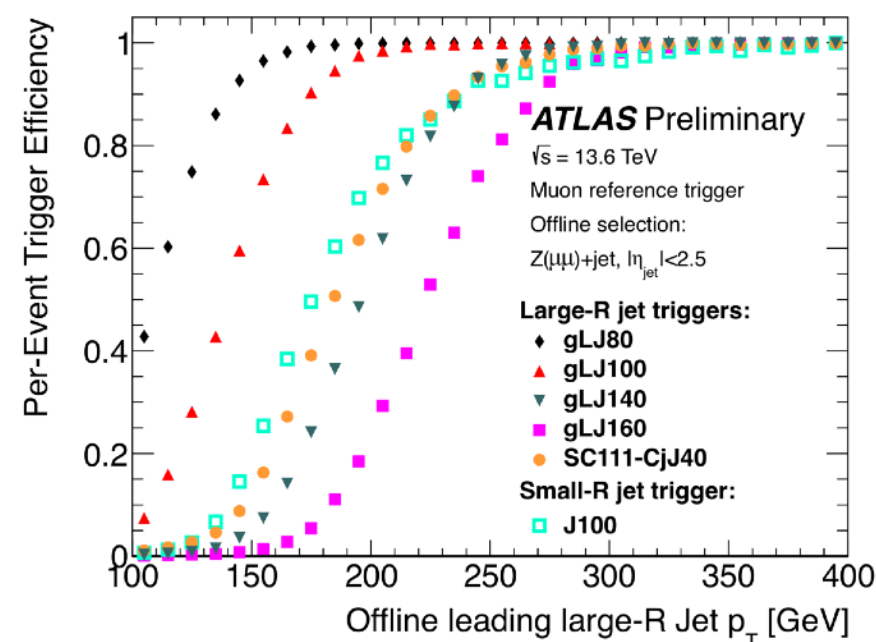
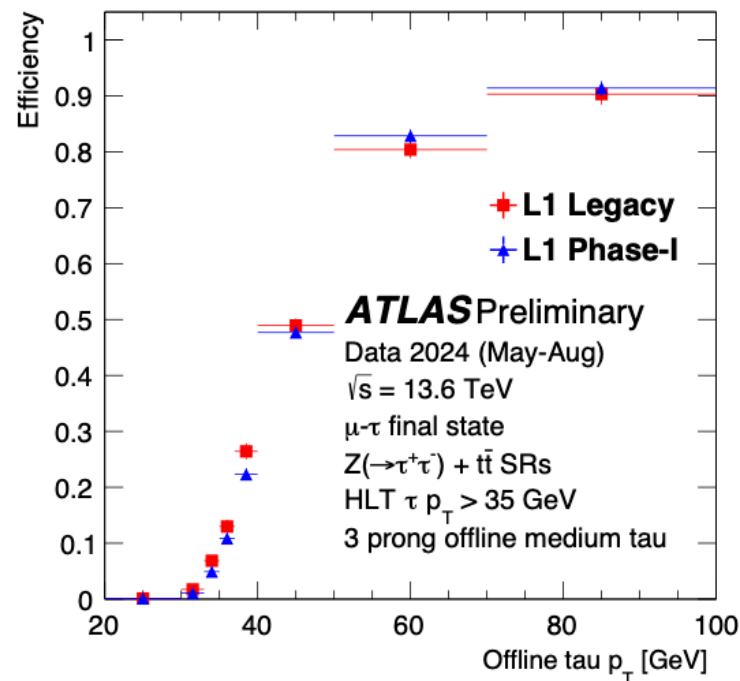
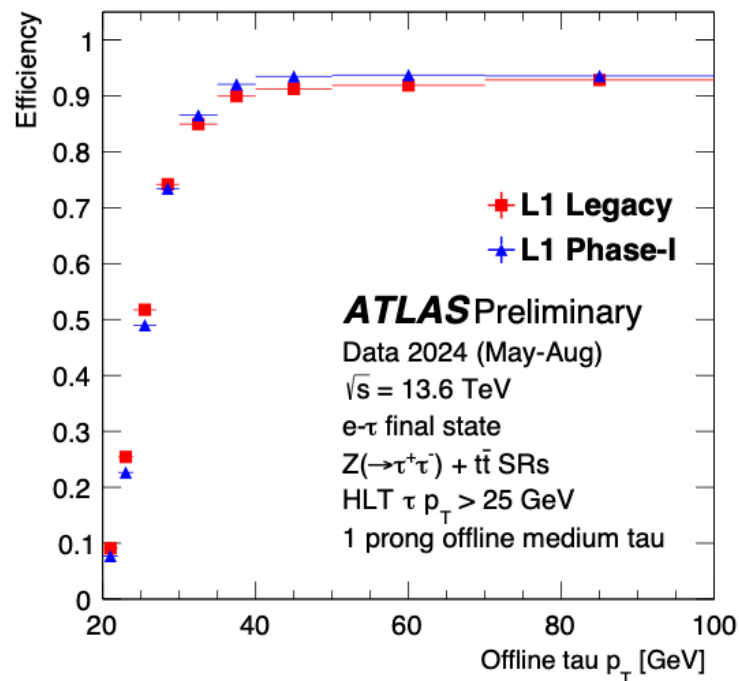
- Level-1 (L1) Calo migration to [Phase-I](#) FPGA based system completed:
 - Improvements over Legacy L1 system already seen in 2023 data taking for electron trigger
- Tau/Jet triggers migration/validation now finished:
 - Longer time scale due to trigger object complexity and sizeable amount of data to be collected for proper validation



- Decommissioning of Legacy L1 system frees resources for next trigger developments and reduces expert load in maintaining the two systems in parallel

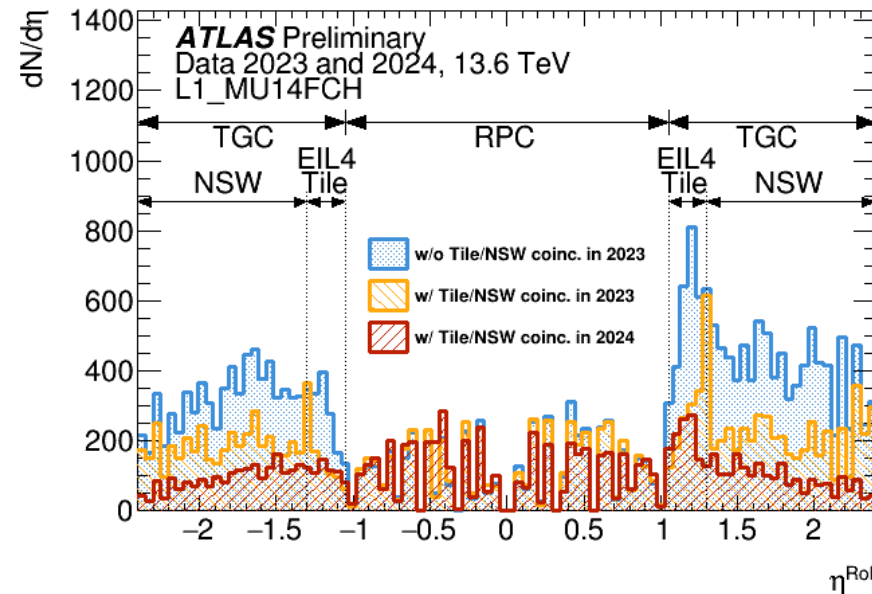
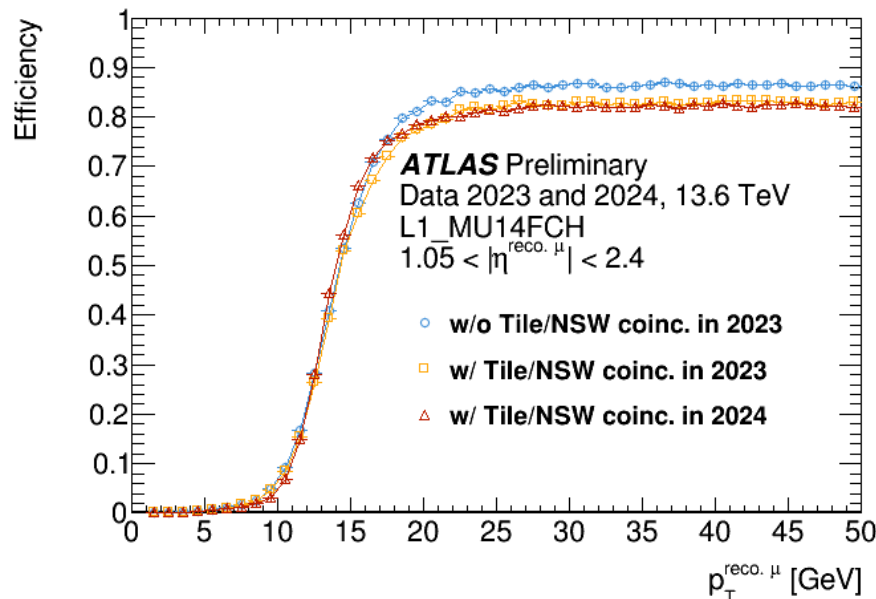
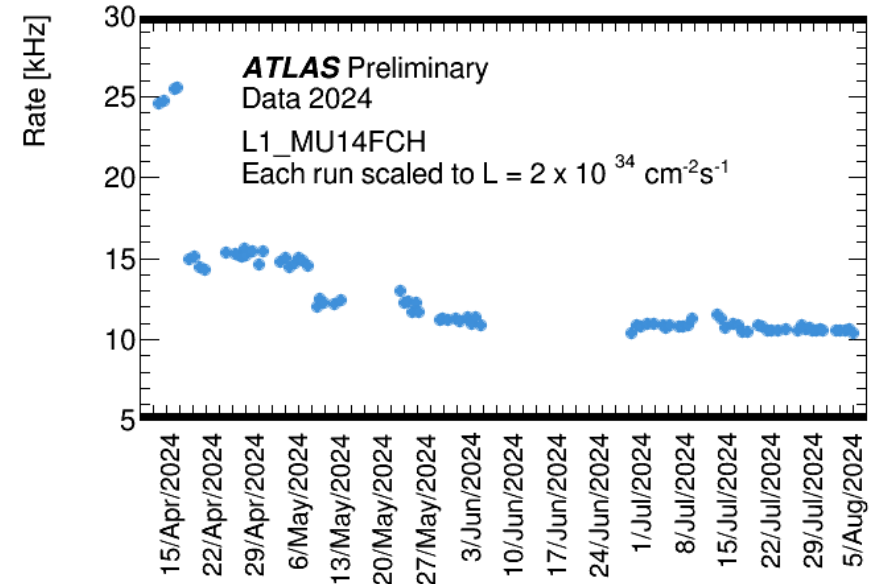
Phase-I L1 latest updates

- L1-Tau involves L1 Topo matching of inputs from eFex and jFex systems for high trigger efficiency at low rate
 - Tuning of standalone/combined systems is crucial to get best performance
 - Current Phase-1 L1 seeded HLT tau trigger performs better/similar to Legacy L1 seeded trigger
- Native large-R jet algorithm improves the L1 trigger performance for physics analyses using large-R jets
 - Demonstrates that gFEX is fully commissioned and a first round of fine tuning is complete.



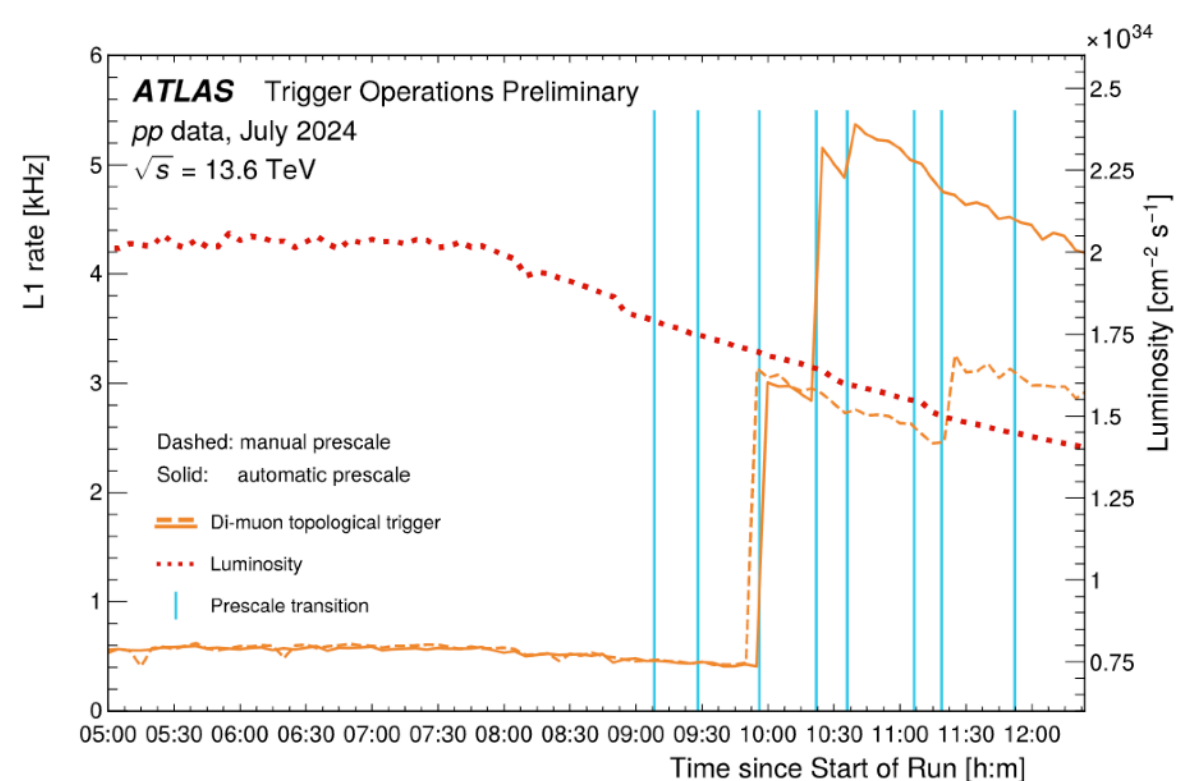
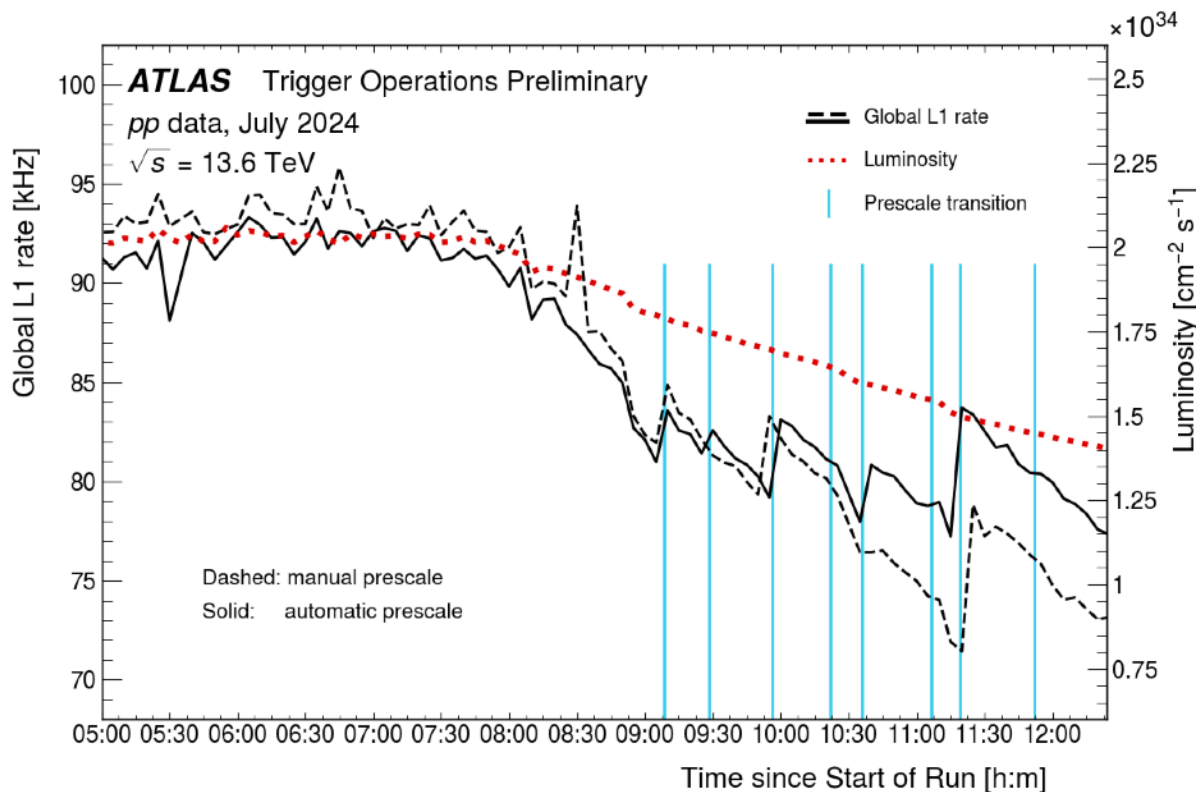
L1 Muon Endcap trigger latest update

- In 2024 reached the activation of all triggers sectors
- Inner coincidence mandatory in 2024 to reach the expected luminosity compatible with maximum L1 rate and dead time
- sTGC PAD and MicroMegs both used in coincidence with the BigWheel, with all sectors reaching more than 95% efficiency
- Overall rate reduction of 15 kHz, including the contribution from the Tile Muon Trigger



End of fill trigger automatised optimisation strategy

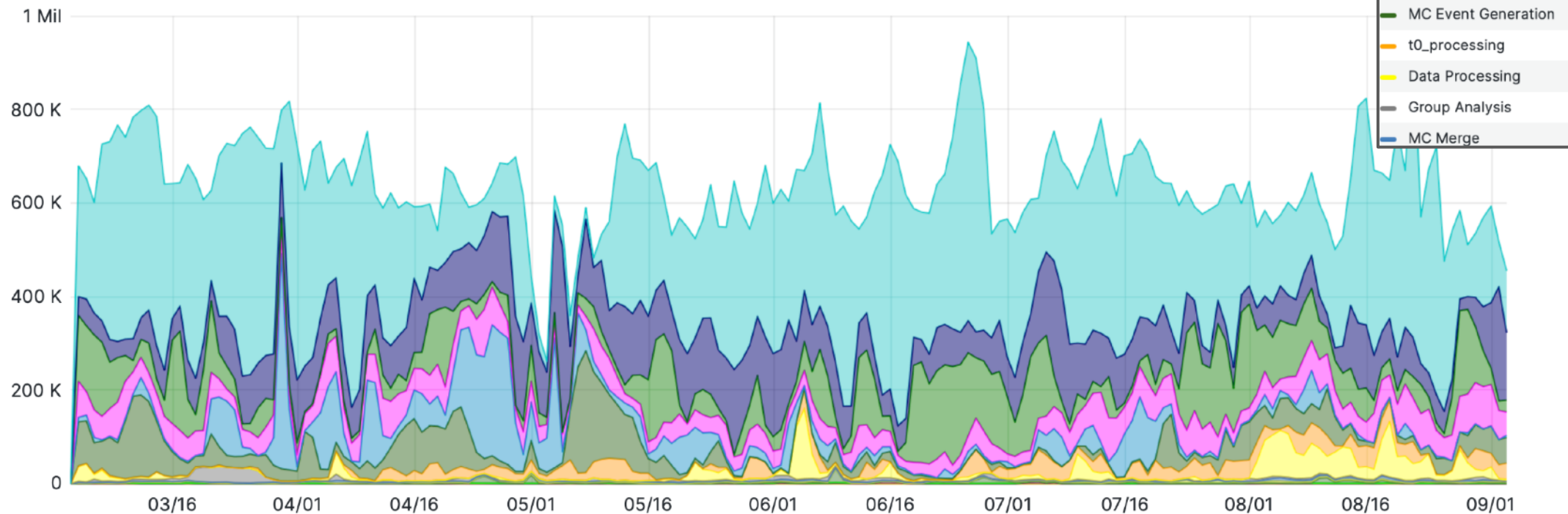
- As a run progresses the delivered luminosity decreases since less colliding protons in each bunch
 - Luminosity levelling is no longer effective
- Due to the lower luminosity, the rate of the various triggers drops creating “space” towards the end of run
 - Increase the rate of previously pre-scaled trigger chains based on physics-driven priority



ATLAS computing and software - resources

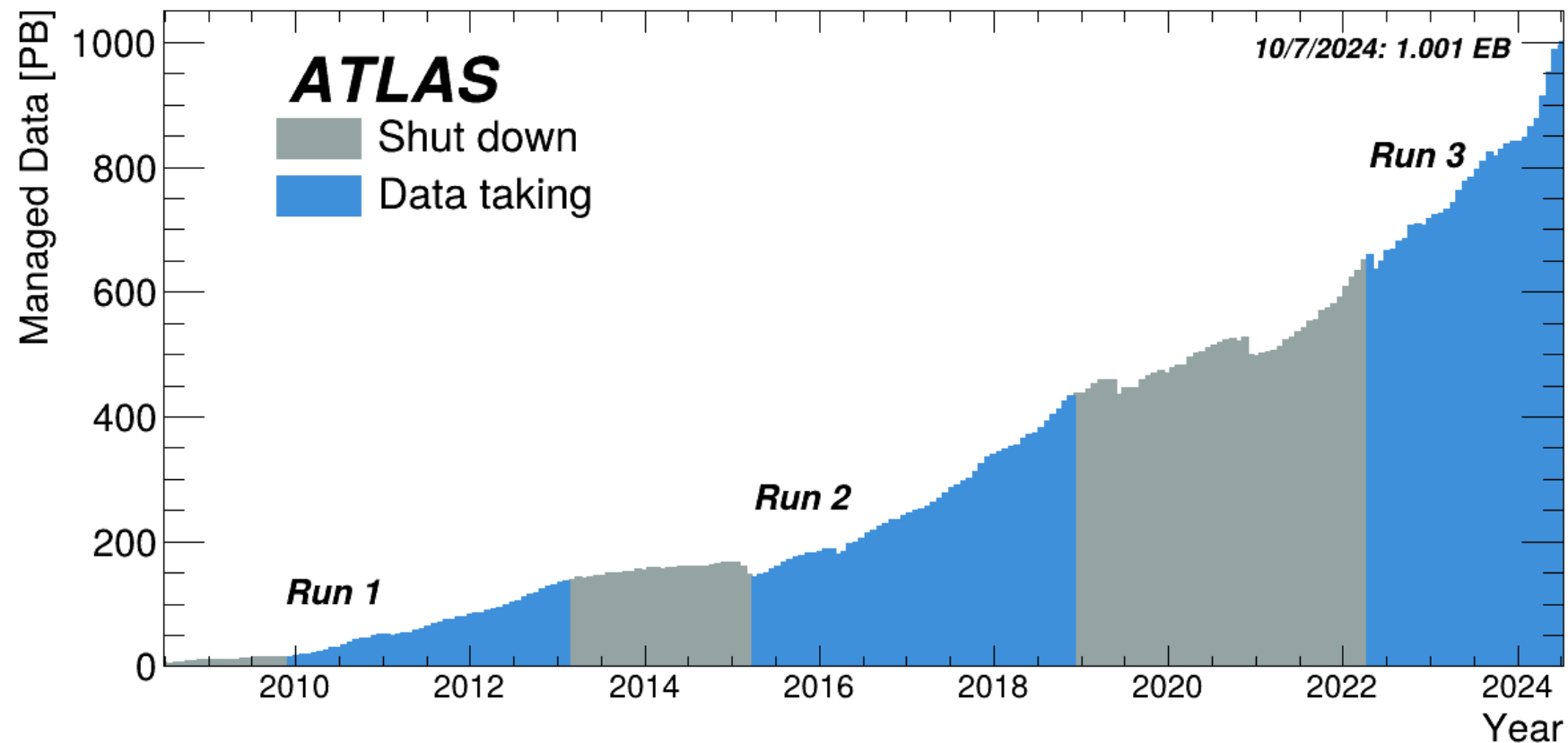
- Running smoothly over the last 6 months
- Major MC23 campaign for 2022, 2023, and 2024 data (digi+reco underway for 2024 data)
- Run3 data reprocessing with improved muon alignment started on August 1st and almost complete
- Power saving ARM processors running routinely; recent peaks up to ~20k cores worldwide
 - ATLAS is the first experiment to accept ARM as part of 2026 pledge

Slots of Running jobs by ADC activity ⓘ



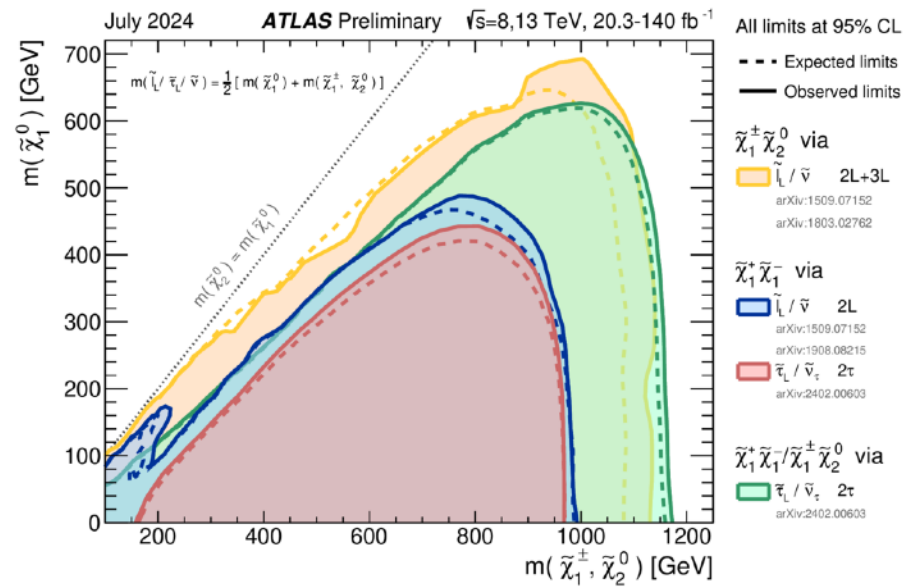
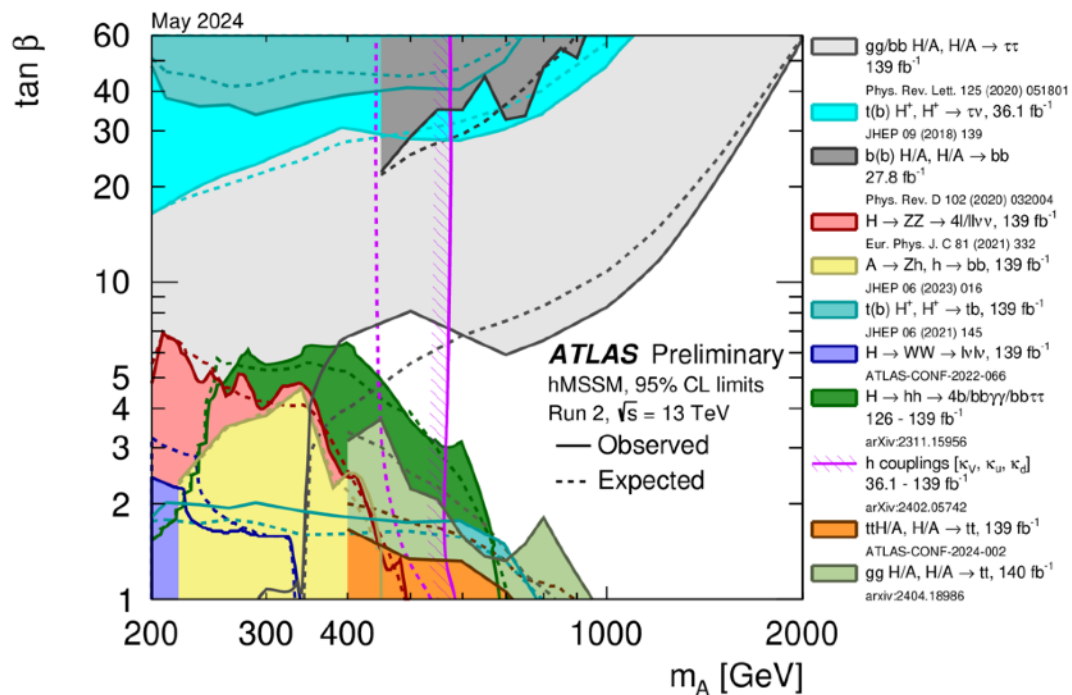
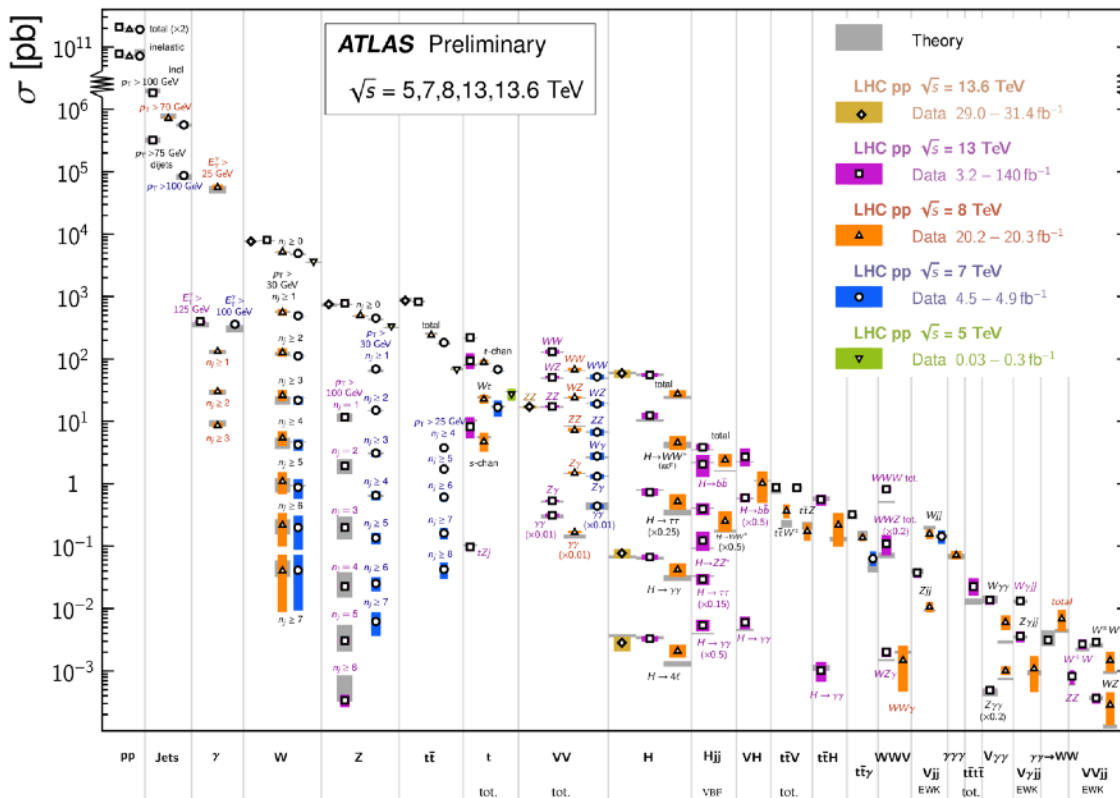
ATLAS computing and software - storage

- Passed 1 Exabyte of Rucio managed data in early July, including both disk and tape storage
- Regular application of lifetime model and obsoletions campaigns to manage space
- Extended effort to move to resource saving common data format across physics analyses



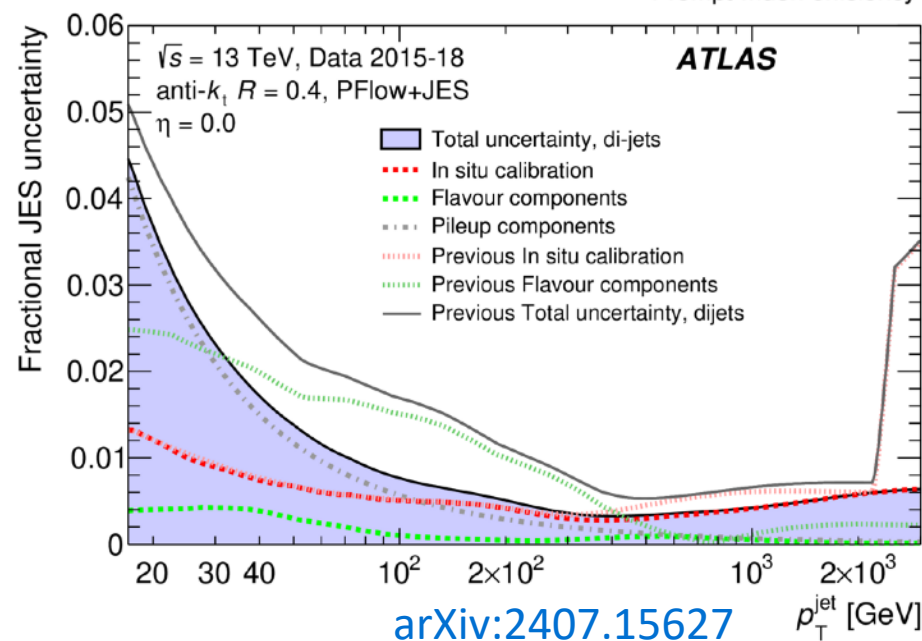
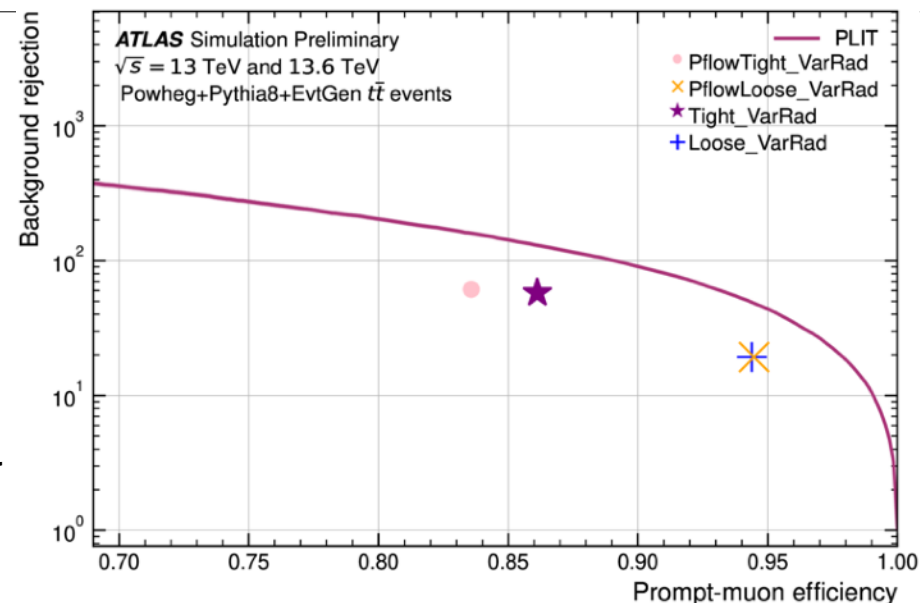
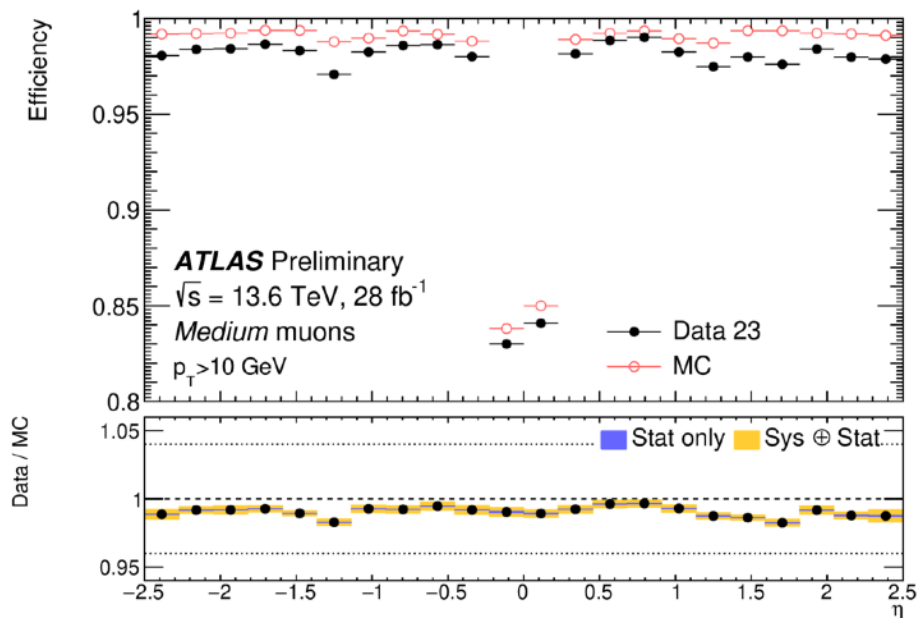
- Since the last LHCC meeting
 - 37 papers submitted to journals
 - 4 conference notes
 - 4 pub notes
- 97 papers released in 2024 so far
- Next slides will show only a subset of the latest results

Standard Model Production Cross Section Measurements



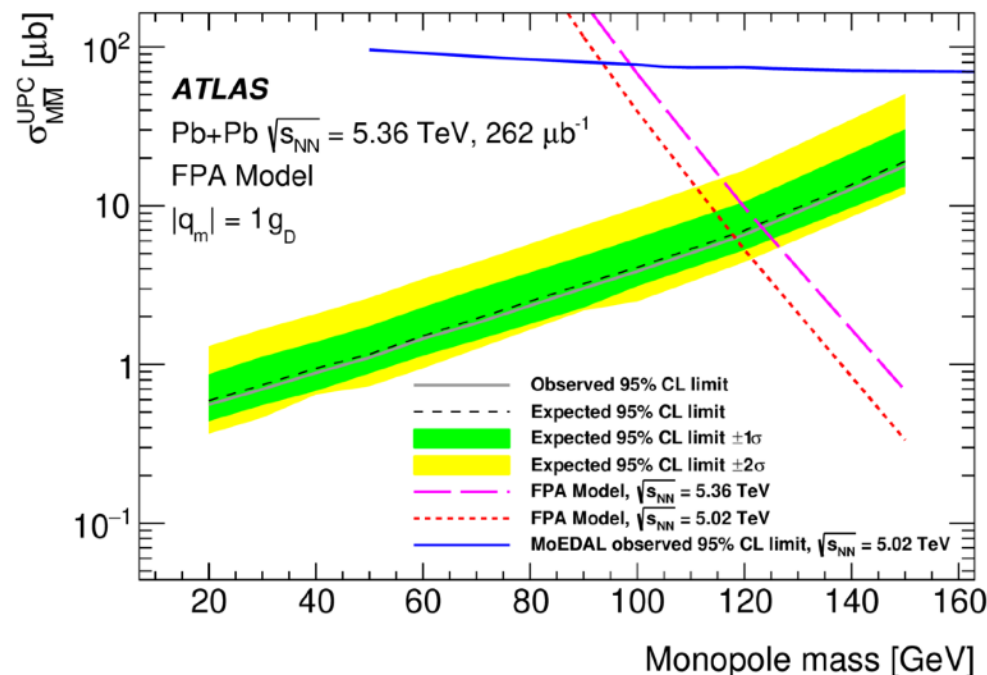
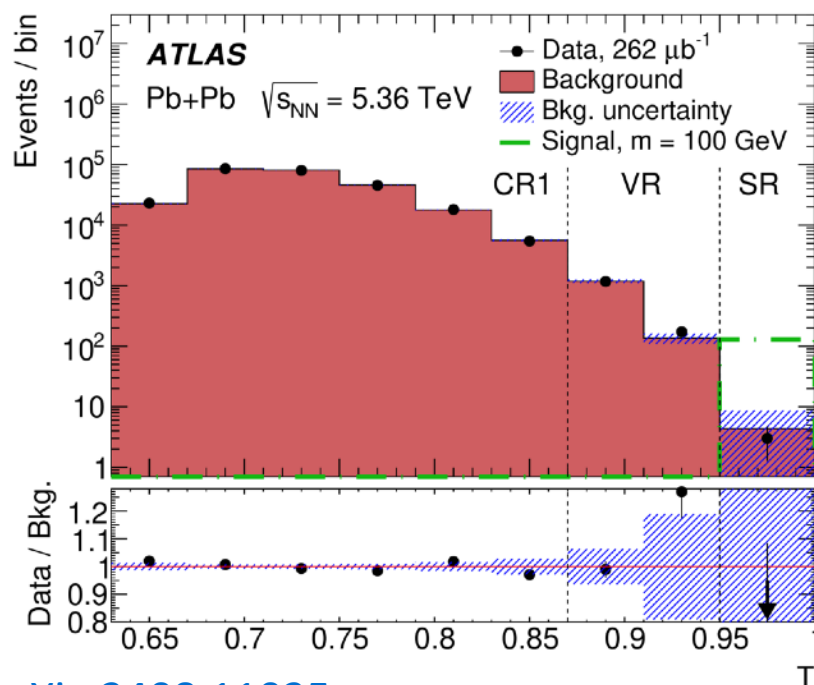
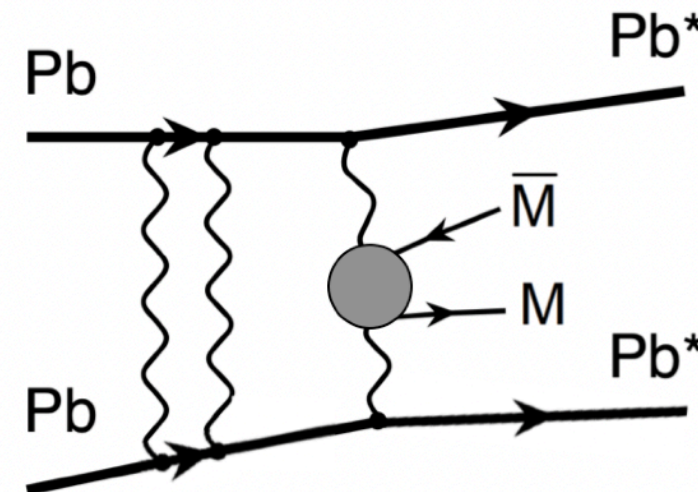
Combined performance measurements

- Particle reconstruction and identification are key elements for improvements in physics results and opening to previously unexplored phase spaces
- Improvements coming from:
 - New/updated ML techniques
 - Updated Data/MC correction factors with Run3 data
 - Systematic uncertainty size reduction



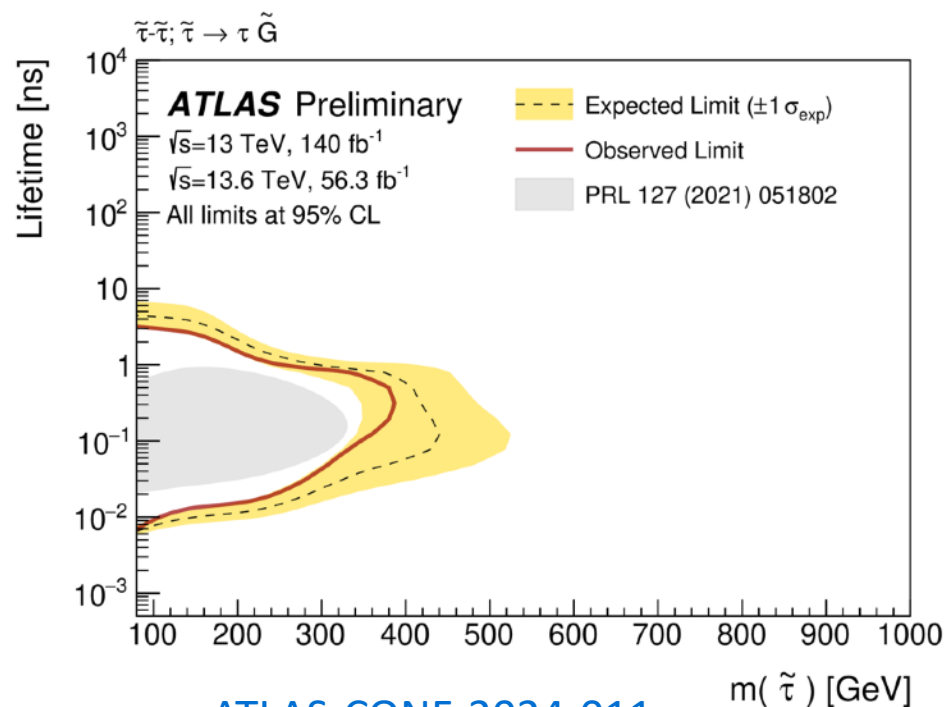
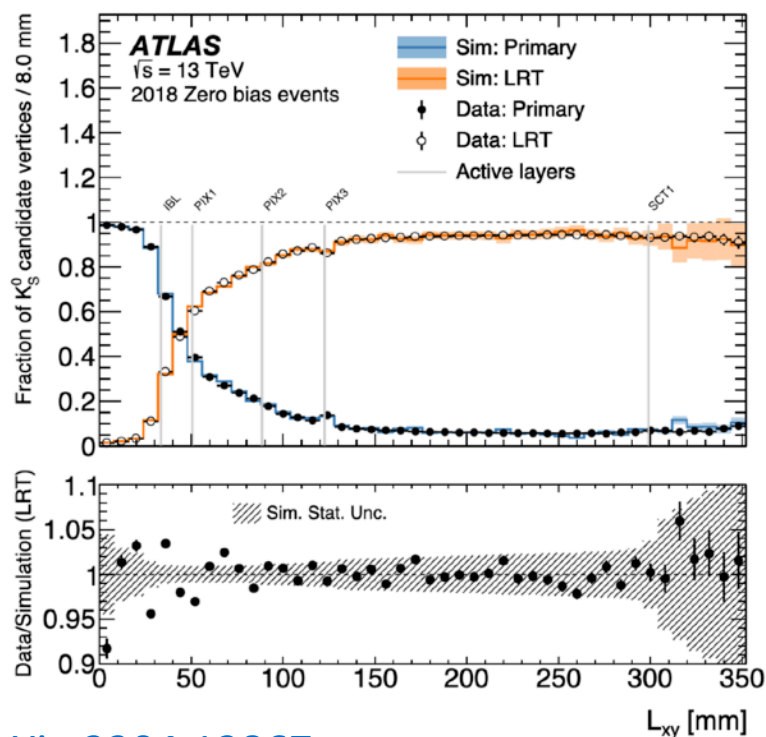
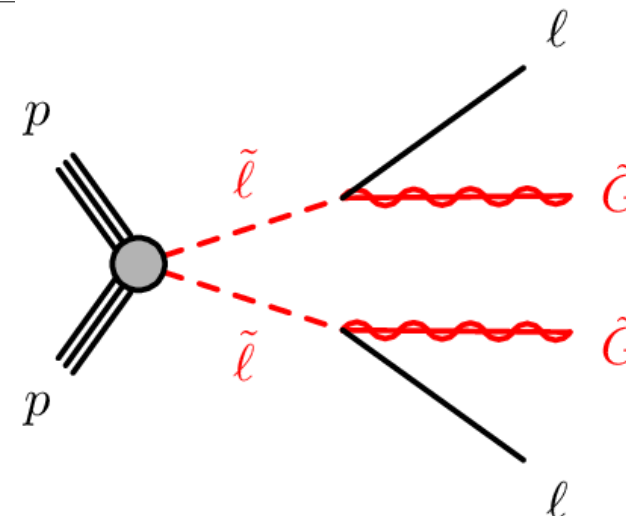
Magnetic monopoles in Ultra-Peripheral lead collisions

- Ultra peripheral collisions (UPC) in lead-lead provide quasi-real photons
- Use UPC to search for magnetic monopole pair production ($M\bar{M}$)
 - Use new data collected in 2023, as well as new ZDC detector based trigger
 - Look at high pixel activity without associated reconstructed tracks
- Excluded magnetic monopoles with mass < 120 GeV
- Improves on the previous cross-section limits reported by MoEDAL



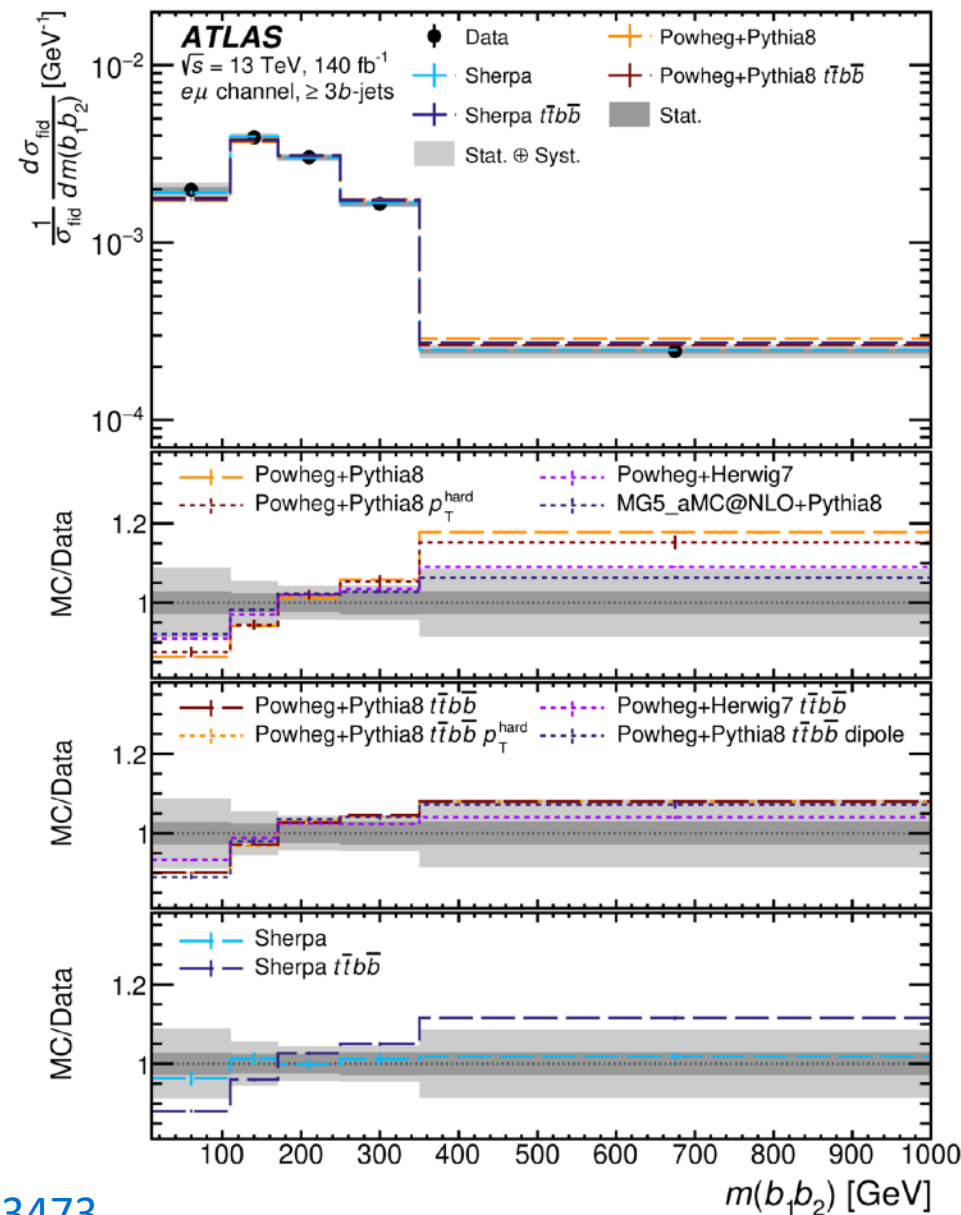
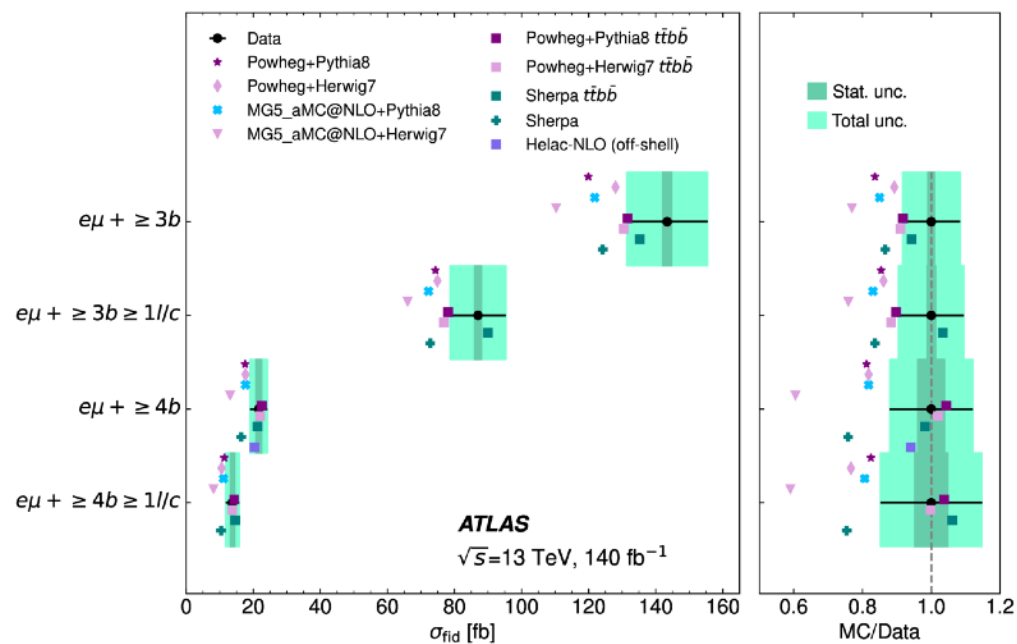
Search for Long Lived Sleptons

- Using Run 3 data (combined with re-analysed Run 2 data) and Large Radius Track Trigger at HLT to improve low- p_T acceptance
- Precision timing information from calorimeter to complement tracking system
- Selectrons, smuons and staus with 0.3 ns lifetime are excluded up to 740 GeV, 840 GeV and 380 GeV, respectively



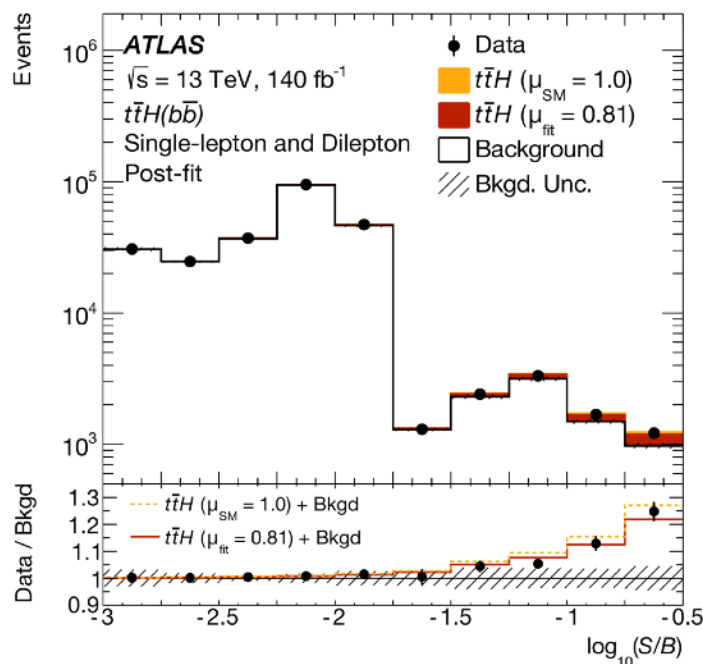
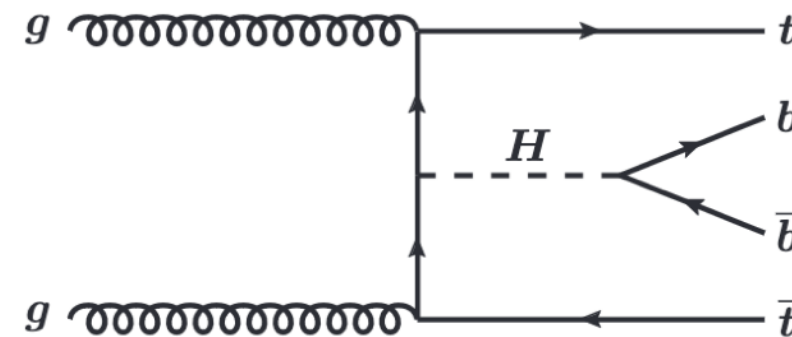
$t\bar{t}$ + b-jets association production cross-section

- Important and extensive measurements to improve theory modelling of this process
 - Provide further improvements for $t\bar{t}H$ measurement
- Fiducial and normalised differential cross section in single lepton (e and μ) channel with 3 or 4 b-jets.
- Precision 10% achieved on several unfolded observables

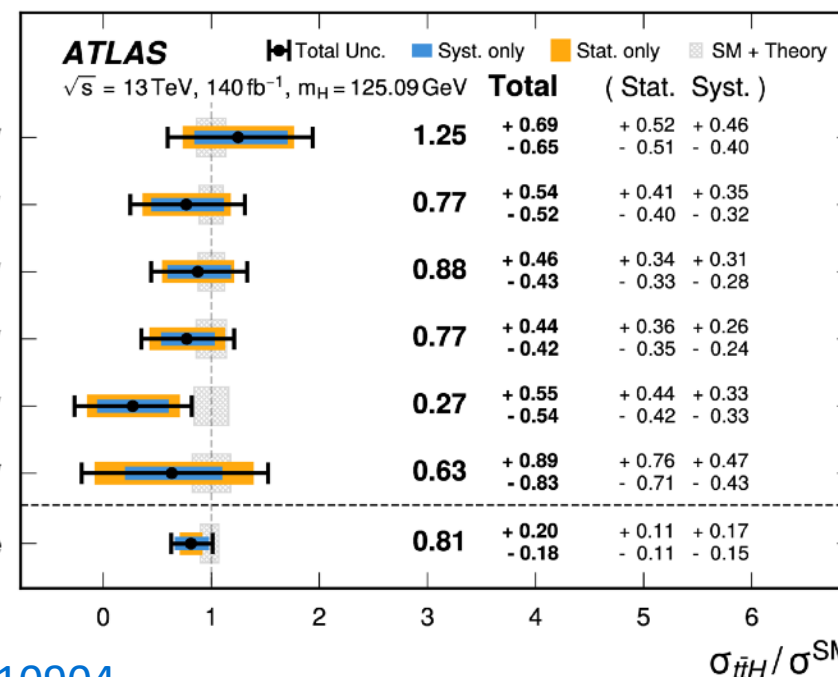


Higgs coupling to heavy flavour, $t\bar{t}H(\rightarrow b\bar{b})$

- Direct probe of top Yukawa coupling
- Major background from $t\bar{t} + b$ -jets
- Advanced neural network to classify the selected collision events
- $t\bar{t}H$ production observed with 4.6σ and total uncertainty improved by $\sim 40\%$ with respect to the [previous measurement](#)
- Cross section measured also in the STXS formalism
 - Measurement dominated by stat. uncertainty for $p_T^H > 300$ GeV



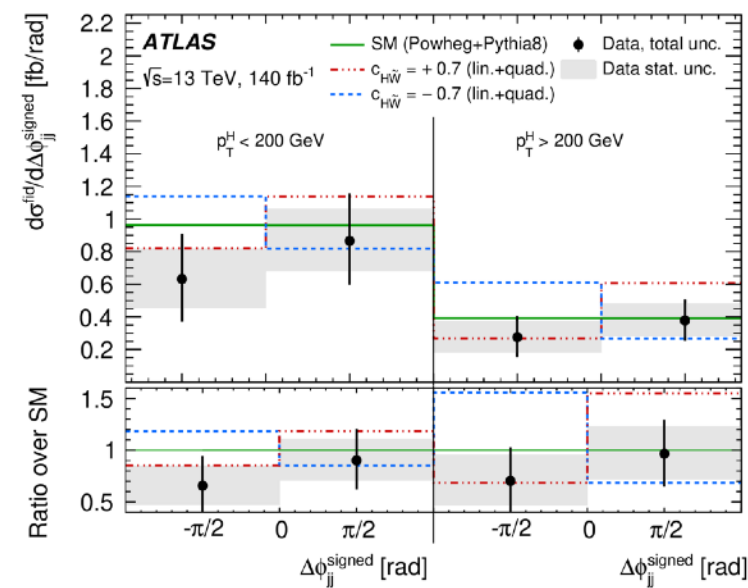
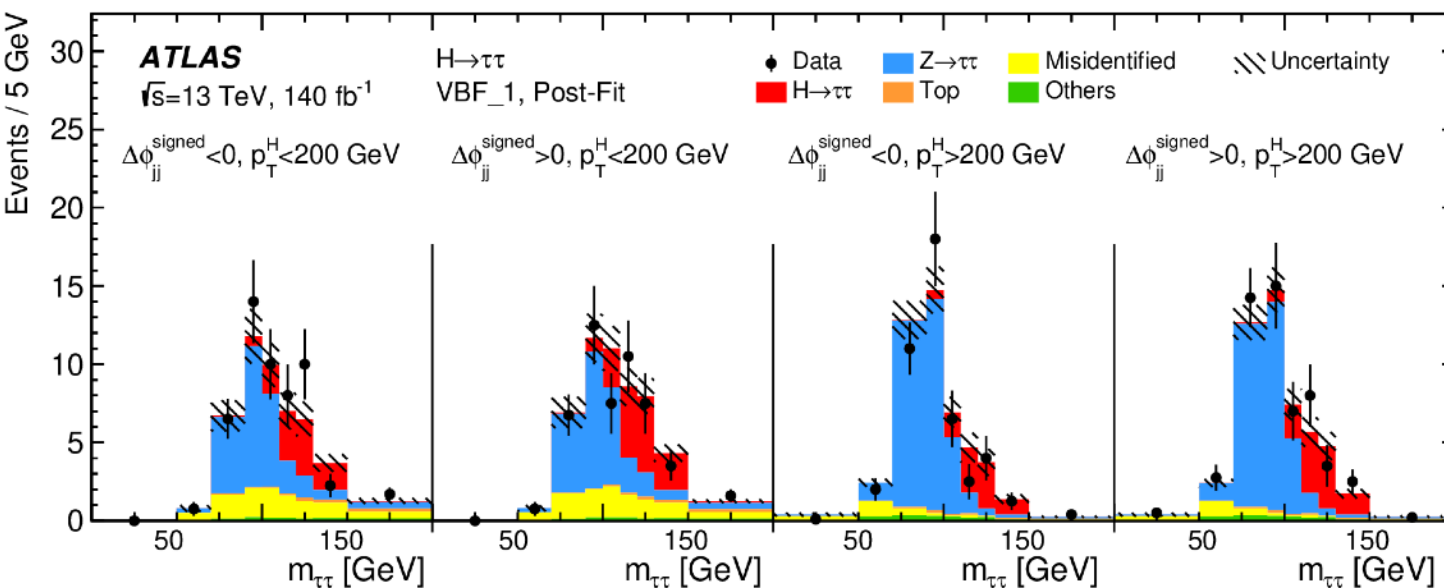
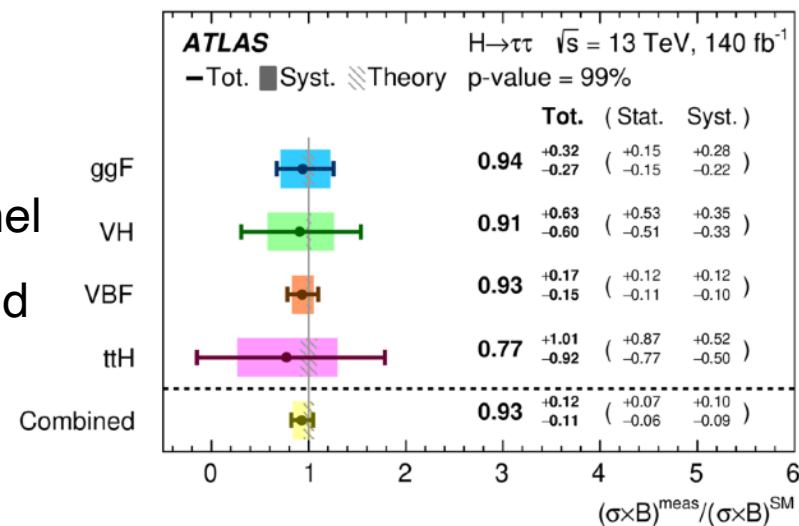
$p_T^H \in [0, 60)$ GeV
 $p_T^H \in [60, 120)$ GeV
 $p_T^H \in [120, 200)$ GeV
 $p_T^H \in [200, 300)$ GeV
 $p_T^H \in [300, 450)$ GeV
 $p_T^H \in [450, \infty)$ GeV
 Inclusive



[arXiv:2407.10904](https://arxiv.org/abs/2407.10904)

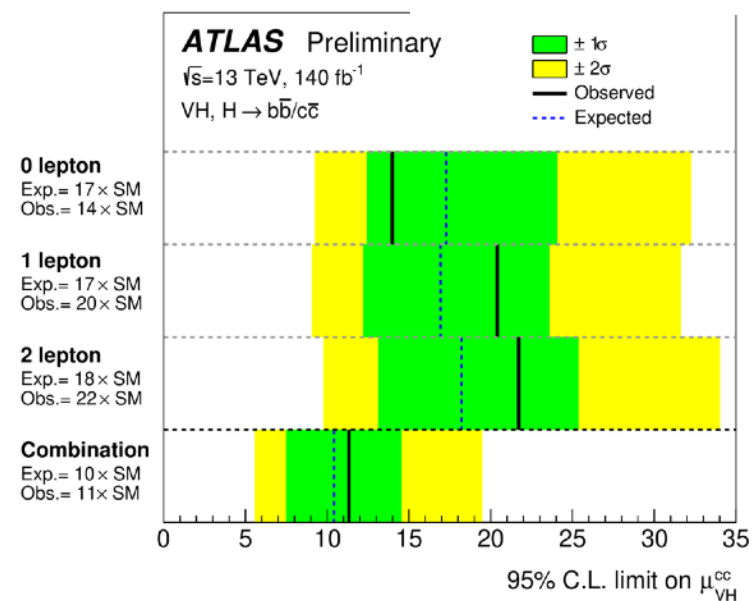
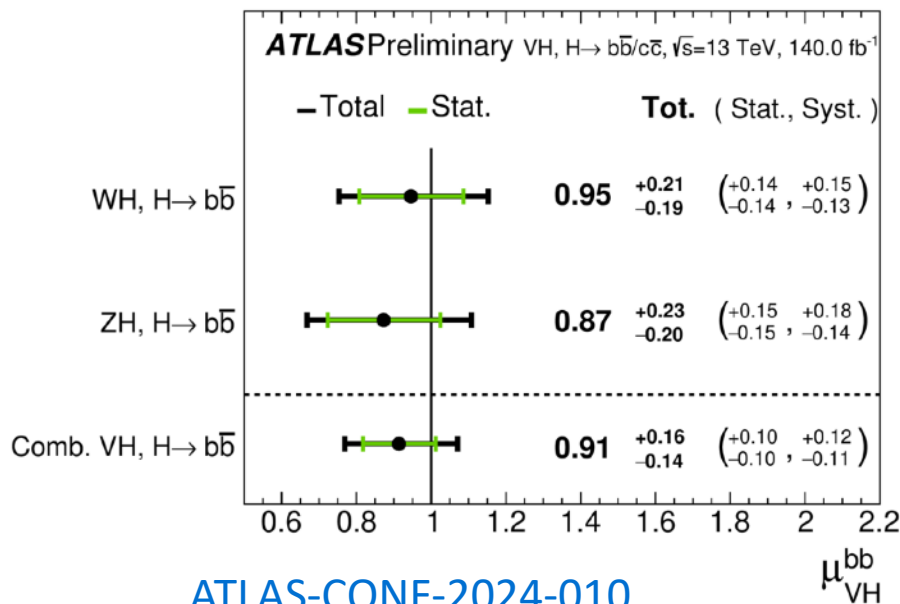
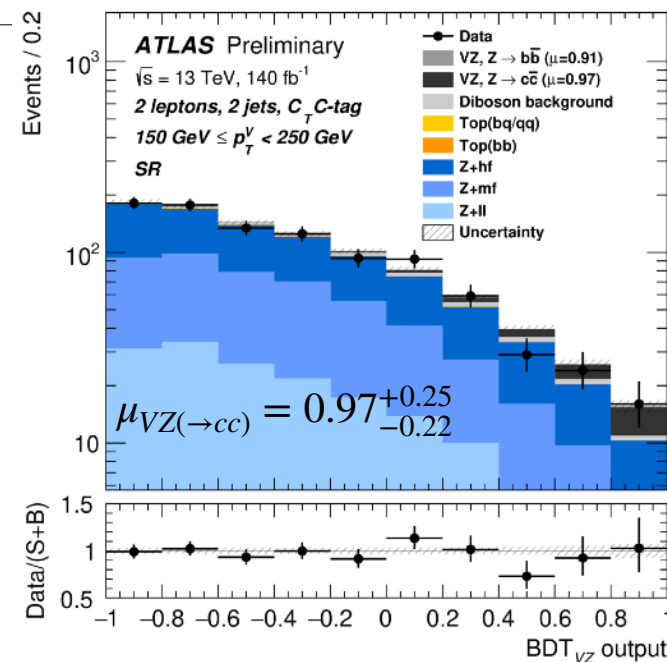
Higgs coupling to third lepton generation, $H \rightarrow \tau\tau$

- Expanding and improving [previous](#) $H \rightarrow \tau\tau$ STXS measurement and include also first differential measurement for VBF Higgs boson production mode in ATLAS in this final state
- Most precise VBF cross-section measurement in a single decay channel
- Performed EFT interpretation in SMEFT framework to constrain CP-odd Wilson coefficients
- 95% C.L. on CP-odd coefficient $C_{H\tilde{W}}$: $[-0.31, +0.88]$ at $\Lambda = 1$ TeV



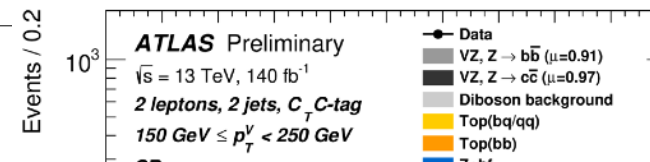
Higgs coupling to second quark generation, $H \rightarrow c\bar{c}$

- Measure $H \rightarrow b\bar{b}$ and $H \rightarrow c\bar{c}$ couplings in VH associated production mode
 - Direct constraints on the charm Yukawa coupling with full Run2 statistics
- Individual production of WH and ZH with $H \rightarrow b\bar{b}$ established with observed (expected) significance of 5.3 (5.5) and 4.9 (5.7) σ
- Limit on $VH(\rightarrow c\bar{c})$ improved by more than factor 2 compared to [previous measurement](#)

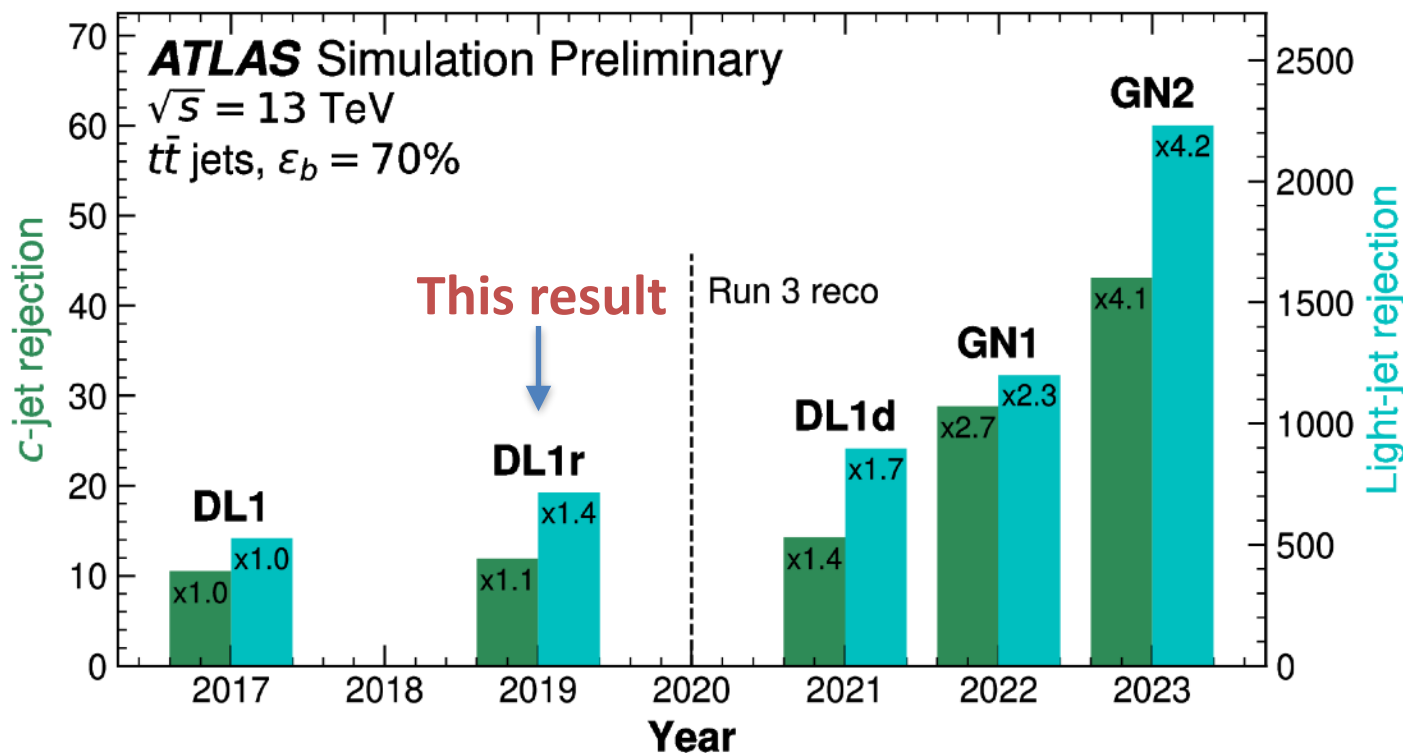


Higgs coupling to second quark generation, $H \rightarrow c\bar{c}$

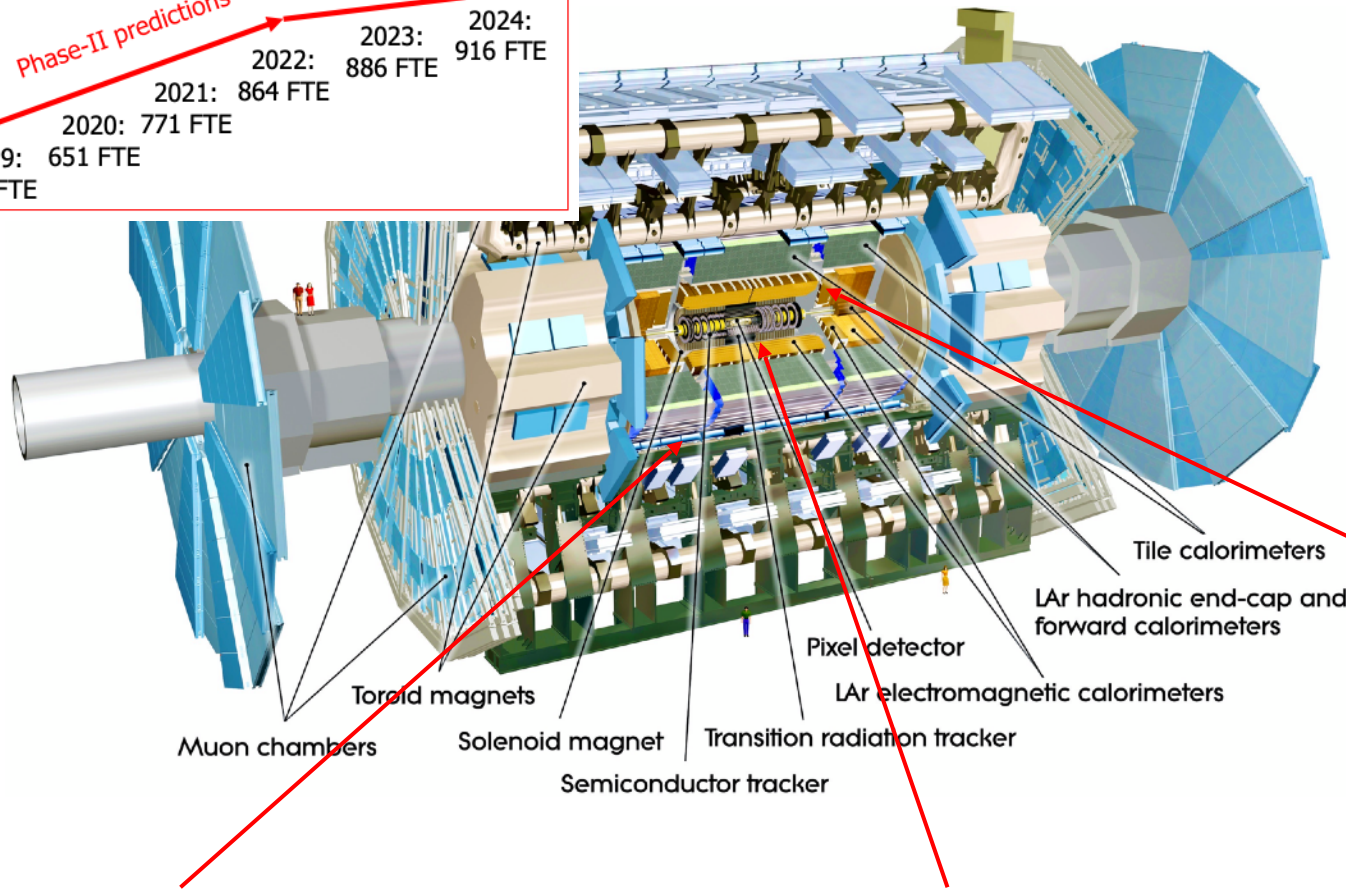
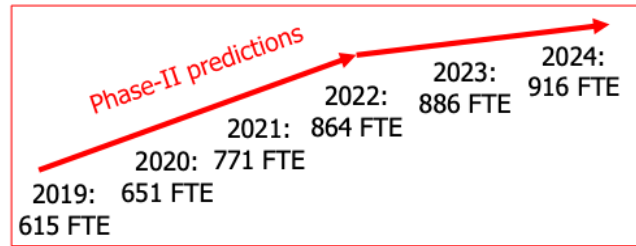
- Measure $H \rightarrow b\bar{b}$ and $H \rightarrow c\bar{c}$ couplings in VH associated production mode



- Expect further improvements in the next analyses due to improved flavour-tagging algorithm



ATLAS Phase-II upgrade



Upgraded Trigger and Data Acquisition system

Level-0 Trigger at 1 MHz
Improved High-Level Trigger (150 kHz full-scan tracking)

Electronics Upgrades

LAr Calorimeter
Tile Calorimeter
Muon system

High Granularity Timing Detector (HGTD)

Forward region ($2.4 < |\eta| < 4.0$)
Low-Gain Avalanche Detectors (LGAD) with 30 ps track resolution

New Muon Chambers

Inner barrel region with new RPC and sMDT detectors

New Inner Tracking Detector (ITk)

All silicon, up to $|\eta| = 4$

Additional small upgrades

Luminosity detectors (1% precision goal)
HL-ZDC

Detailed scope described in 7 TDRs approved by the CERN Research Board in 2017, 2018, 2020

Recent Phase-II project highlights

Huge progress across the board, many parts in production, technical challenges being addressed but schedule is too tight

ITk Pixel

- Pixel production progresses well with sensors, FE ASIC, and hybridisation start with 2 (out of 4) vendors, some bare local supports in production, and some of the services
- Planning to start module production this year; PRRs scheduled this October

ITk Strip

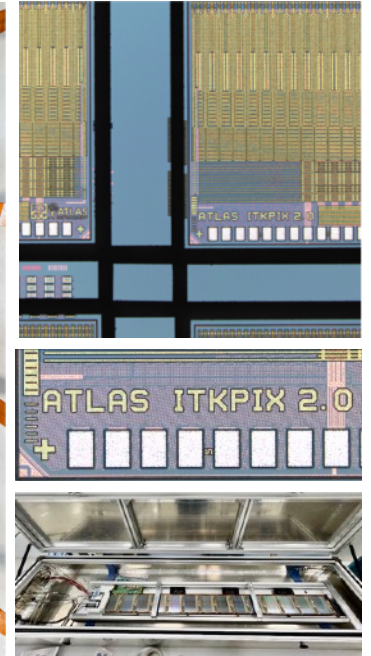
- ASIC and module component in production; sites ready for module production
- Strip sensor fracturing of cold mounted modules under intense follow up
 - Solution with 50 μm kapton interposer being developed
 - Successfully tested for the barrel in half stave (14 modules) at temperature of -70°C ; no evidence of cracks

Production of ITk common items and structures proceeds well

ITk Pixel quad modules



ITkPixV2 wafer



Stave reception test box, SR1

**Interposer = silicon, kapton, CFRP
Glue = SE4445,**



Installation of Itk polymoderator in SR1



Transport of Strip L3 shell to SR1

Recent Phase-II project highlights

LAr Calorimeter

- FE ASICs: Preamp/shaper (ALFE) and ADC (COLUTA) in production, awaiting return of calibration ASICs
- FEB2 v2 with improved power down-conversion circuit tested, PDR soon, then produce miniseries, LASP (off-detector signal processor) prototype design converging

Tile Calorimeter

- Good overall progress (Main Board production, burn-in test, LVPS pre-production, calib. system design, etc)

Timing Detector – HGTD

- Final HGTD readout ASIC (ALTIROC-A) complete pre-production, tests ongoing
- Progress on hybridisation, use thicker sensors to improve thermal bump-bond robustness
- Testing readout integration: modules, detector units, flex tails, Peripheral Electronics Boards

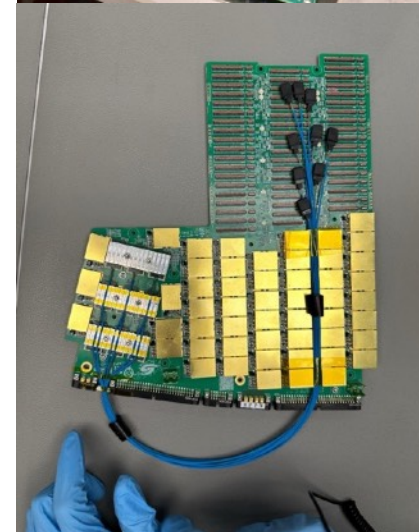
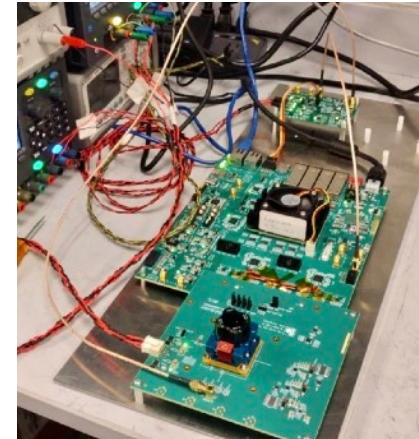
Muon

- sMDT chamber production complete, good progress on electronics, moving towards PRRs
- RPC mechanics tender closed, singlet production launched, gas gap leaks being investigated; RPC readout ASIC production with 2 variants with TDC and the disc-only backup delivered and under test

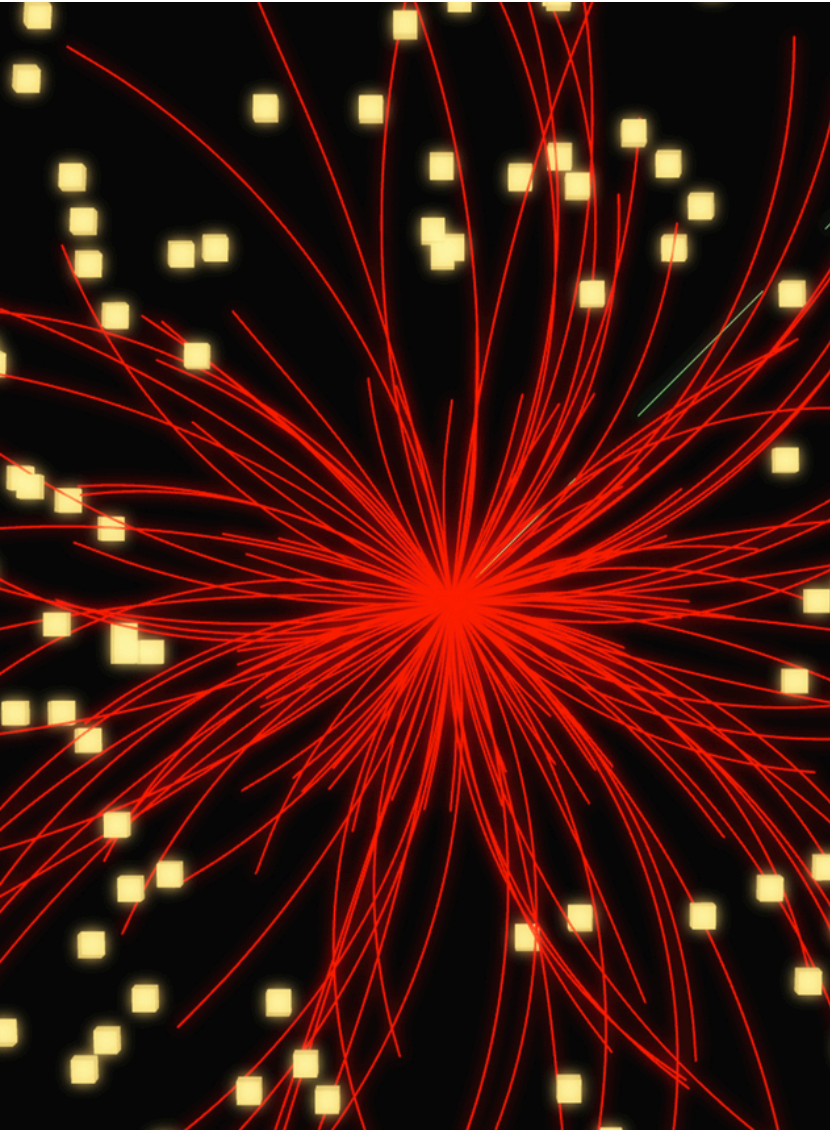
TDAQ

- Good overall progress, negative float due to insufficient effort in NSW trigger processor, new effort found, need to consolidate
- NextGenTrigger project: many hires done, work has started (see [here](#) for a recent status update on the work packages)

FEB2 mass testing board



HGTD PEB prototype



News

Tags:
[open data](#),
[computing](#)

ATLAS releases 65 TB of open data for research

Explore over 7 billion LHC collision events – from home

1 July 2024 | By [Katarina Anthony](#)

The ATLAS Experiment at CERN has made two years' worth of scientific data available to the public for research purposes. [The data](#) include recordings of proton–proton collisions from the Large Hadron Collider (LHC) at a collision energy of 13 TeV. This is the first time that ATLAS has released data on this scale, and it marks a significant milestone in terms of public access and utilisation of LHC data.

“Open access is a core value of CERN and the ATLAS Collaboration,” says Andreas Hoecker, ATLAS Spokesperson. “Since its beginning, ATLAS has strived to make its results fully accessible and reusable through open access archives such as [arXiv](#) and [HepData](#). ATLAS has routinely released open data for educational purposes. Now, we’re taking it one step further — inviting everyone to explore the data that led to our discoveries.”

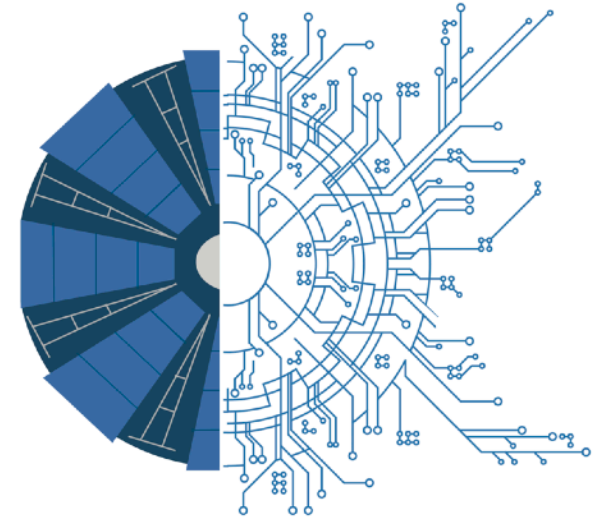
Released under the [Creative Commons CC0 waiver](#), ATLAS has made public all the data collected by the experiment during the 2015 and 2016 proton–proton operation of the LHC. This is approximately 65 TB of data, representing over 7 billion LHC collision events. In addition, ATLAS has released 2 billion events of simulated “Monte Carlo” data, which are essential for carrying out a physics analysis.

Today's release underscores the ATLAS Collaboration's long-standing commitment to open access principles.

```
if (taus.size() > 0)  
{
```

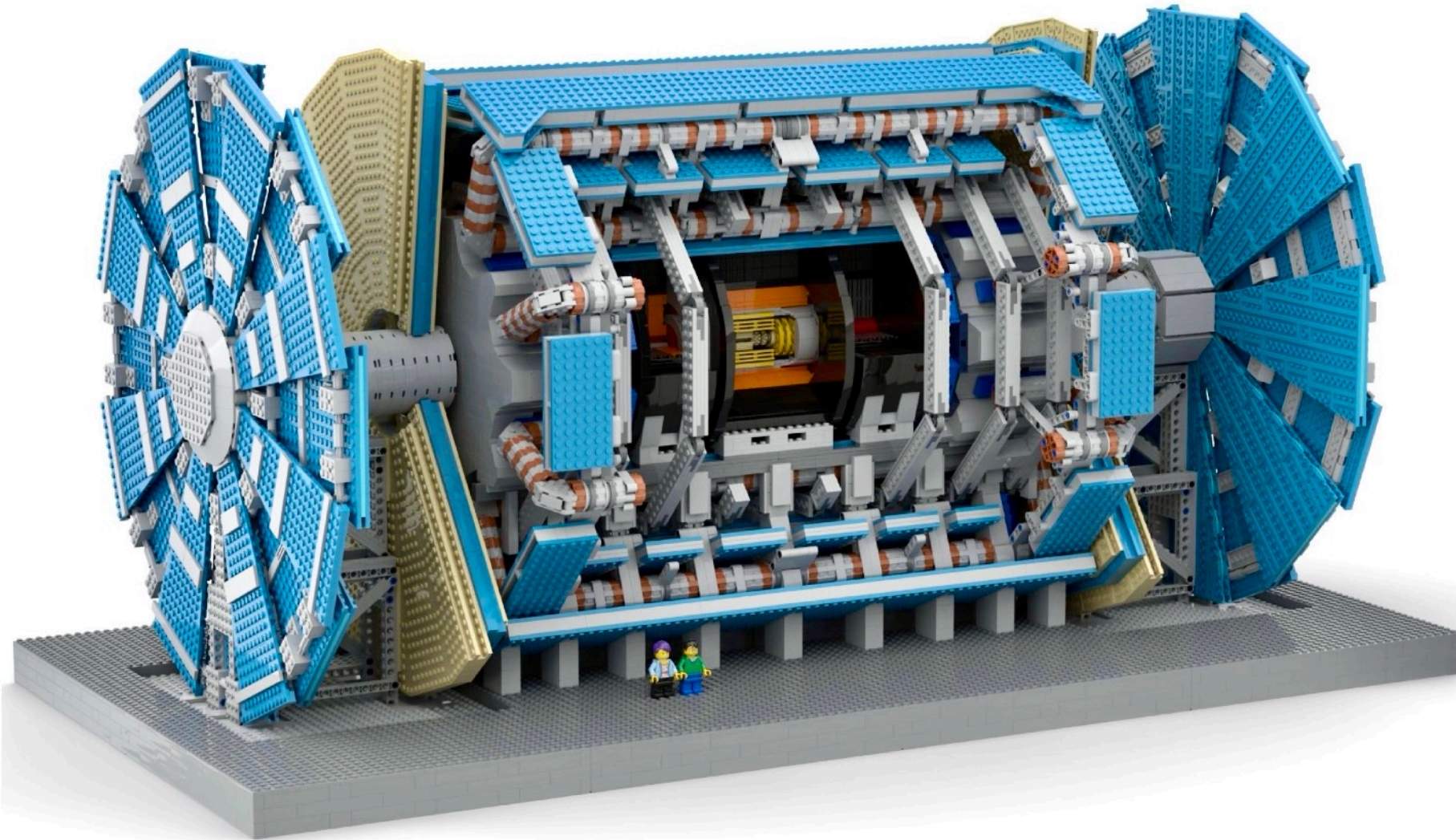
Conclusion

- Data taking progressing smoothly in 2024:
 - (As of 11 Sep) Collected 91.6 fb^{-1} of data with no hardware/software limitations
 - Levelling at $\langle \mu \rangle = 64$ thanks to Phase-I upgrades
- Many important physics results since the last LHCC meeting:
 - Capitalising on Run3 improvements in trigger and reconstruction for monopoles and long lived particles
 - Significantly improved results in Higgs boson coupling to fermions
- ATLAS progressing with high priority on Phase-II upgrades, crucial production activities ongoing, and in the meantime ...



ATLAS
FUELED BY ML/AI

The LEGO HL-LHC ATLAS Detector



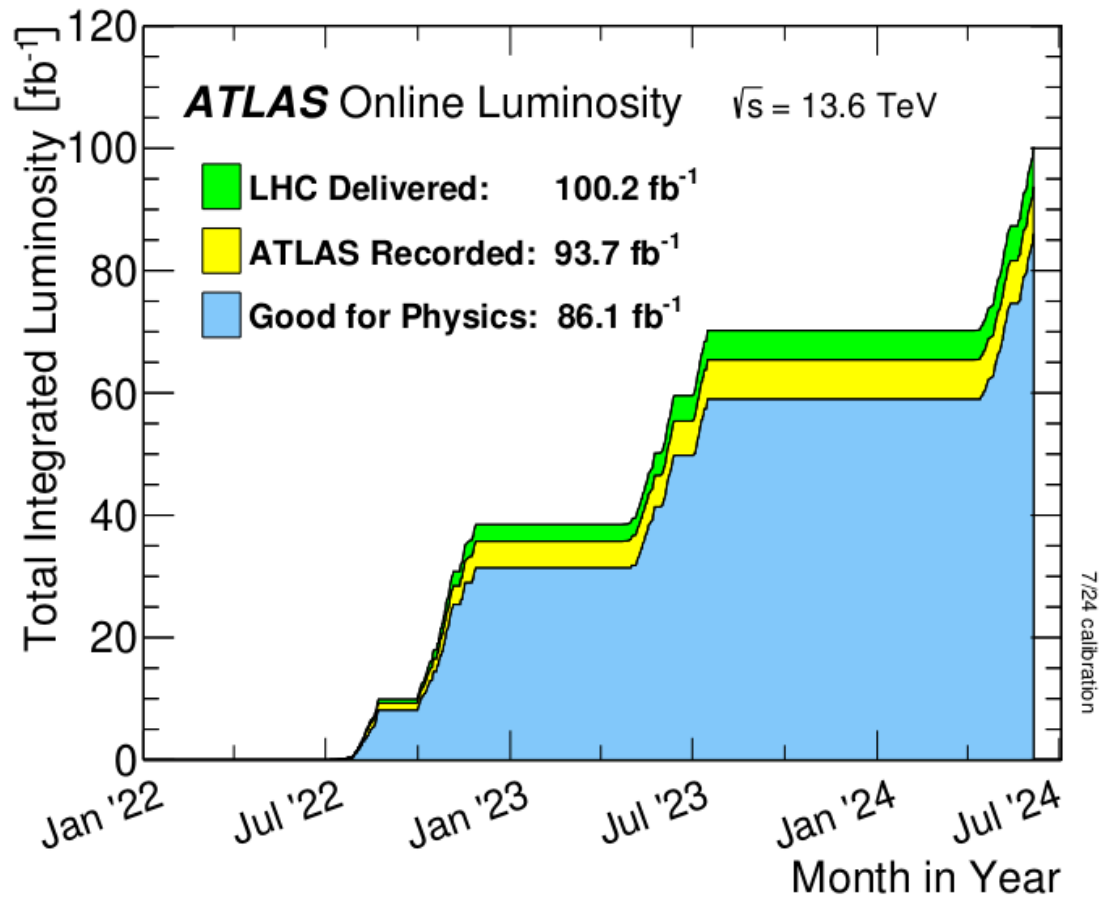
A new ATLAS LEGO model of the Phase-II ATLAS detector (following the pioneering first ATLAS LEGO model of the current detector):

- Hyper-accurate 1:50 scale, more than 100 cm long, 50 cm wide
- 20,188 pieces, 29.5 kg weight
- Manual with 2,015 steps on over 1,180 pages
- Three day building event proved very popular with Sheffield department staff

Thanks a lot for your attention



2024 data taking efficiency



ATLAS pp Run-3: 2024 until 5 June

Trigger	Inner Tracker			Calorimeters		Muon Spectrometer			Magnets		Global	
	Pixel	SCT	TRT	LAr	Tile	MDT	RPC	TGC	Solenoid	Toroid	Lumi calib.	Other
L1+HLT	99.88	99.25	99.66	100	99.87	99.98	99.95	99.75	100	99.82	99.60	100

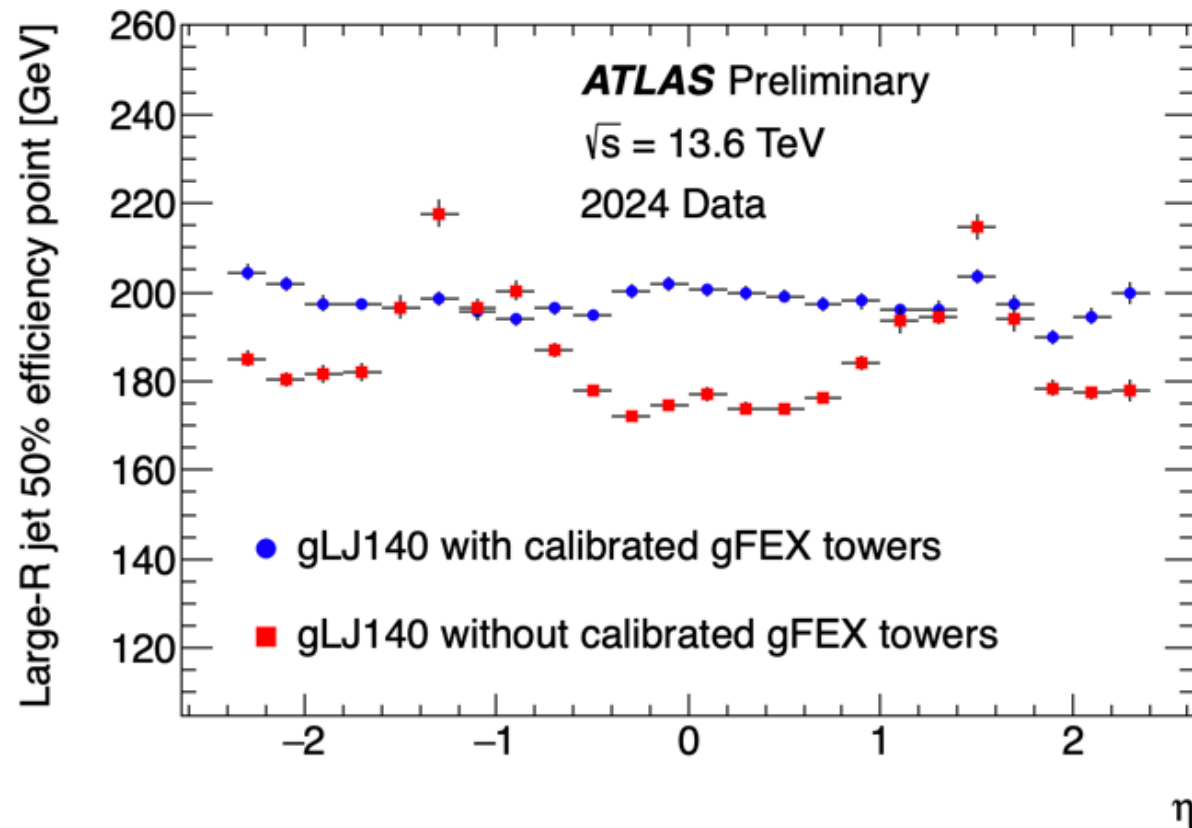
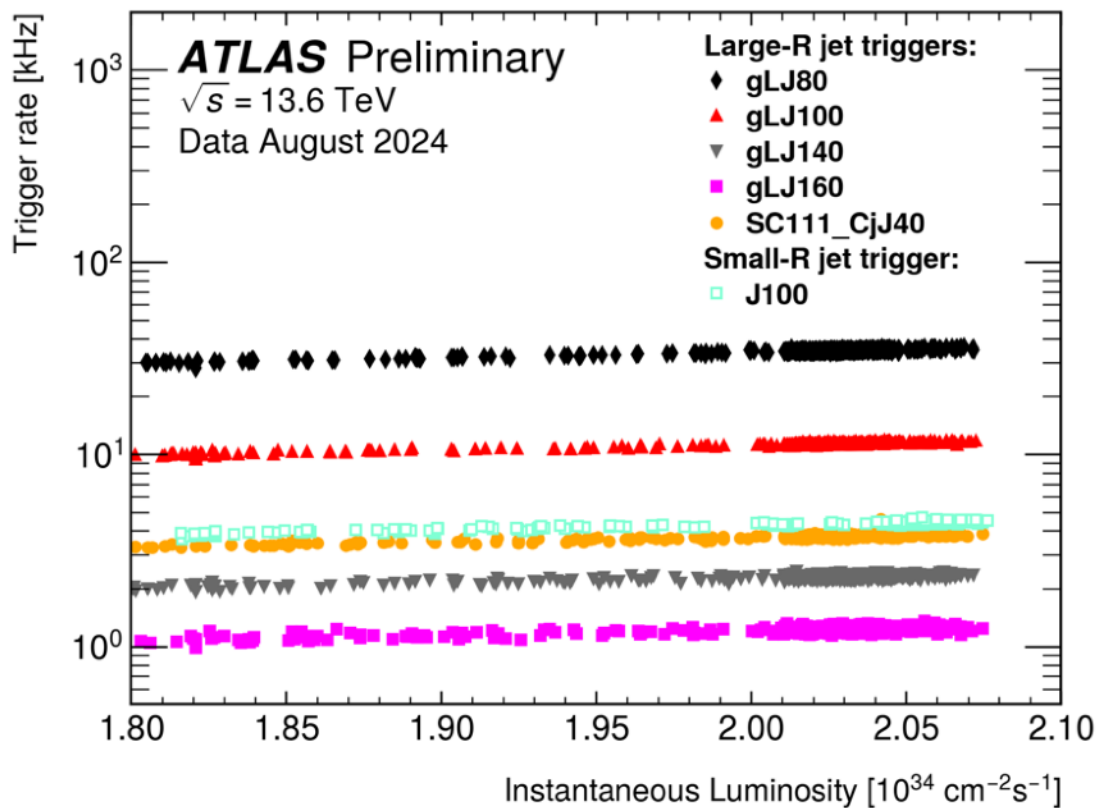
Good for physics: 97.73% (27.1 fb⁻¹)

Luminosity weighted relative detector uptime and good data quality efficiencies (in %) during stable beam in pp collision physics runs at $\sqrt{s}=13.6$ TeV for the 2024 Run-3 period until 5 June, corresponding to a delivered integrated luminosity of 29.1 fb⁻¹ and a recorded integrated luminosity of 27.7 fb⁻¹. Runs with specialized physics goals or non-standard running conditions are not considered and thus not included in the denominator of the efficiency calculation.

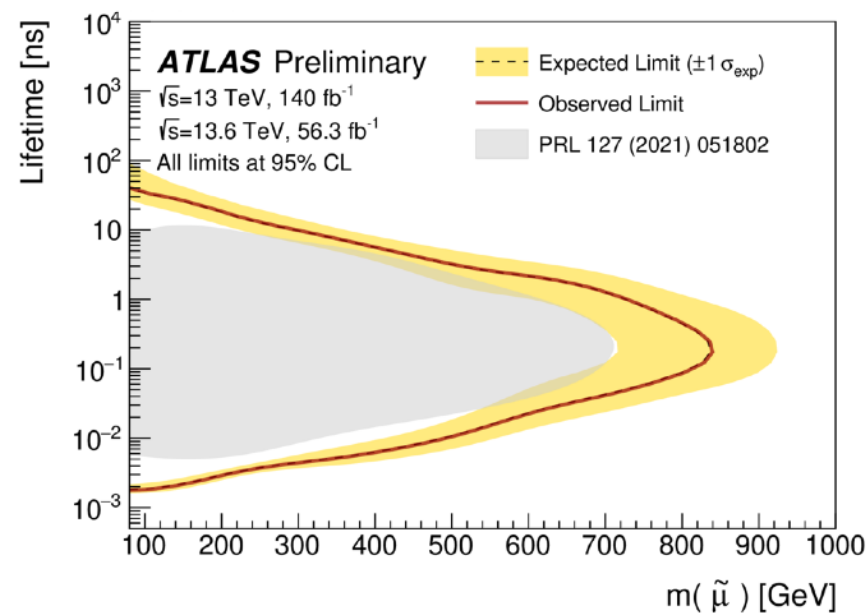
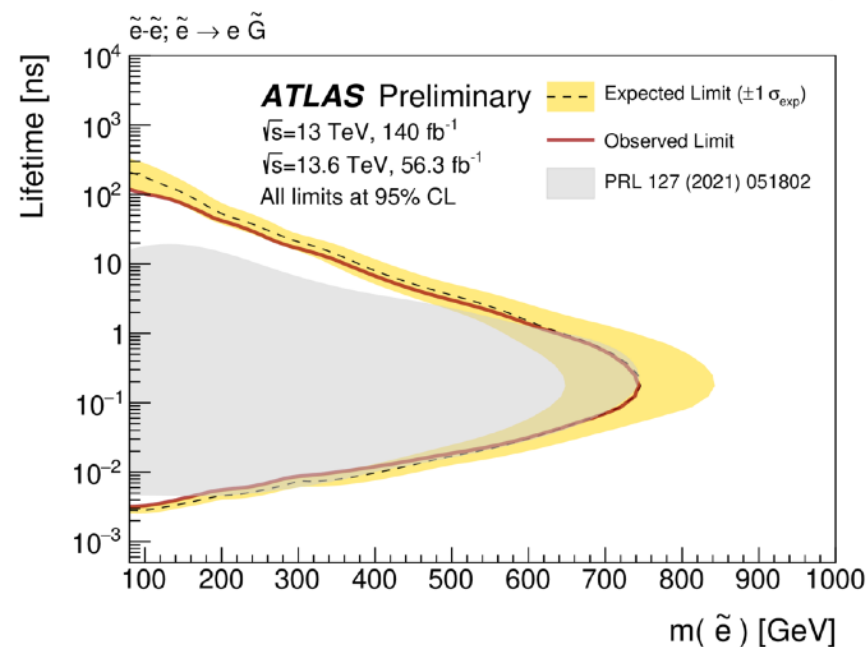
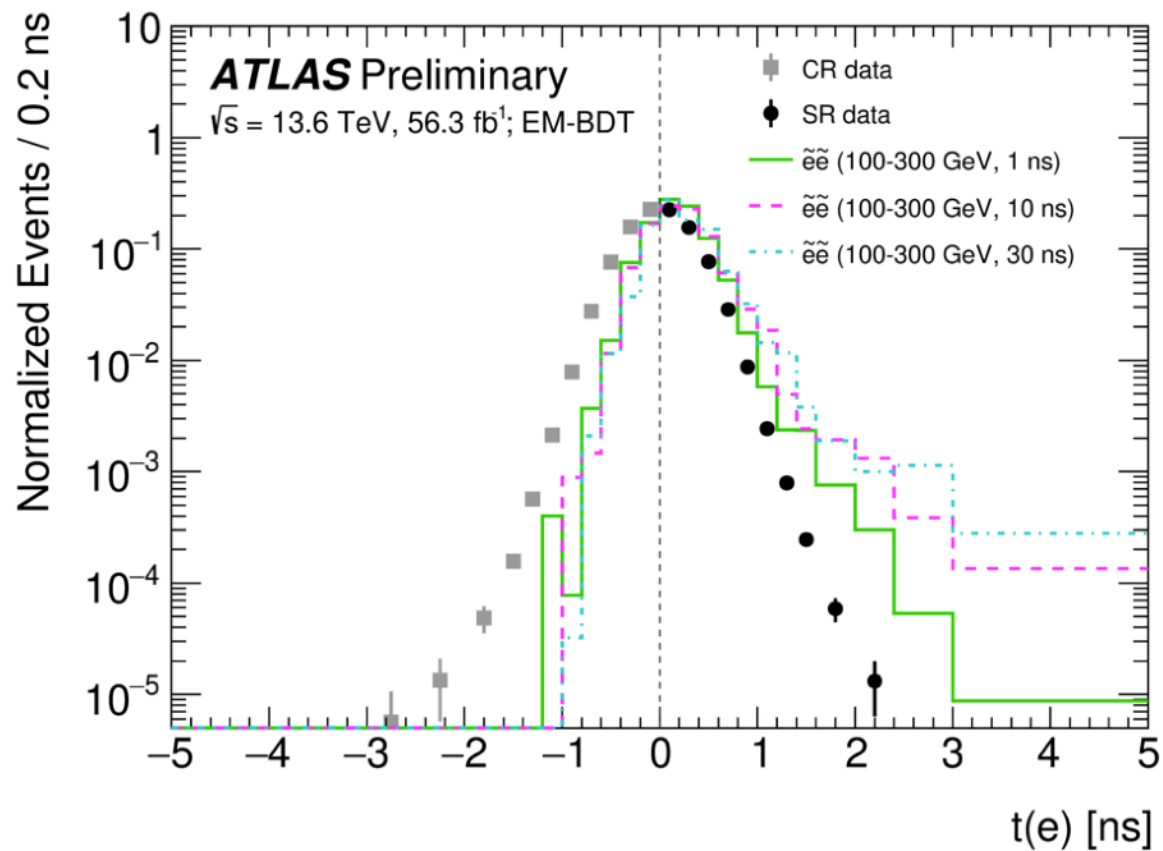
Dedicated luminosity calibration activities during LHC fills used 0.40% of recorded data in 2024 until 5 June and are included in the inefficiency. When the stable beam flag is raised, the tracking detectors undergo a so-called "warm start", which includes a ramp of the high-voltage and turning on the pre-amplifiers for the Pixel system. The inefficiency due to this, as well as the DAQ inefficiency, are not included in the table above, but accounted for in the ATLAS recording efficiency.

The luminosity good for physics is 27.1 fb⁻¹. This is applicable to analyses not relying on b-jet triggers.

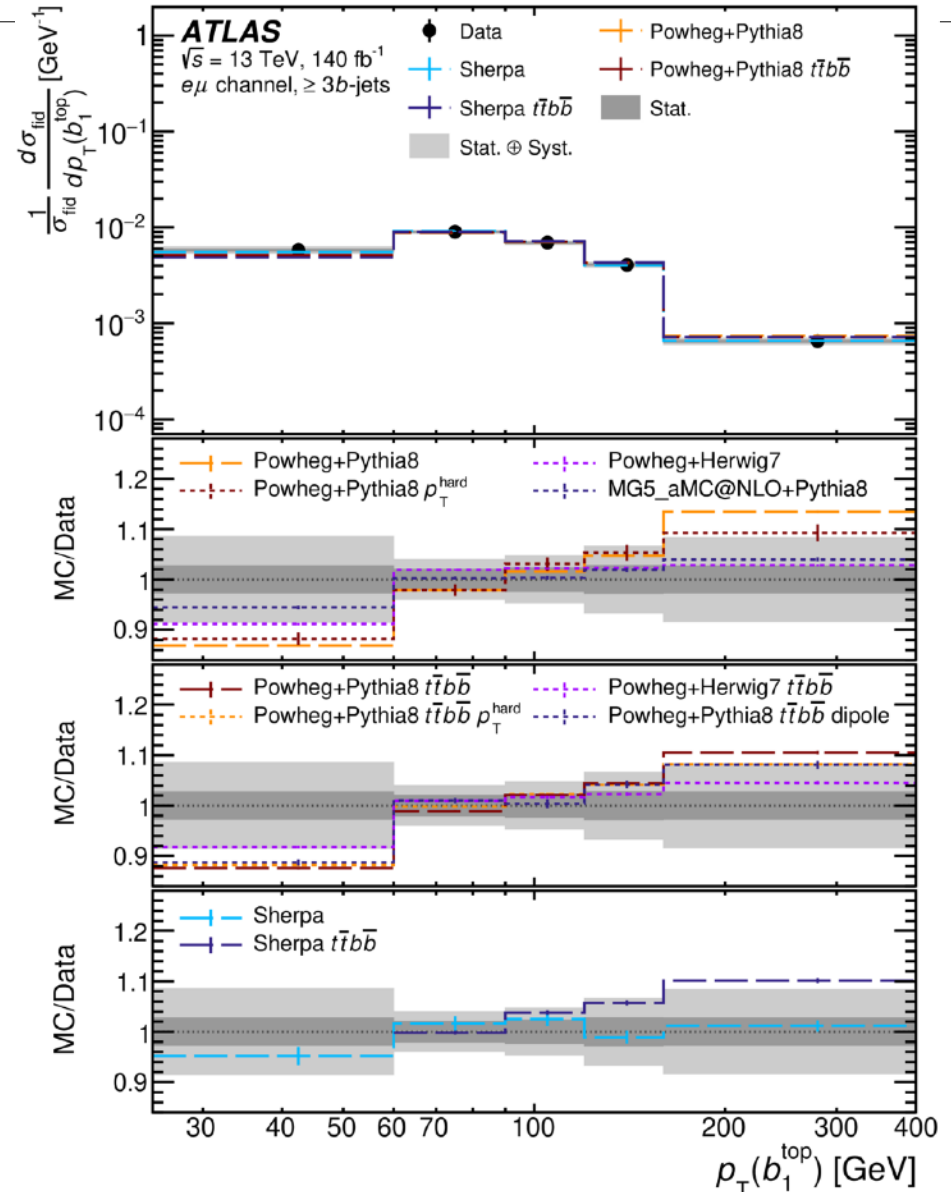
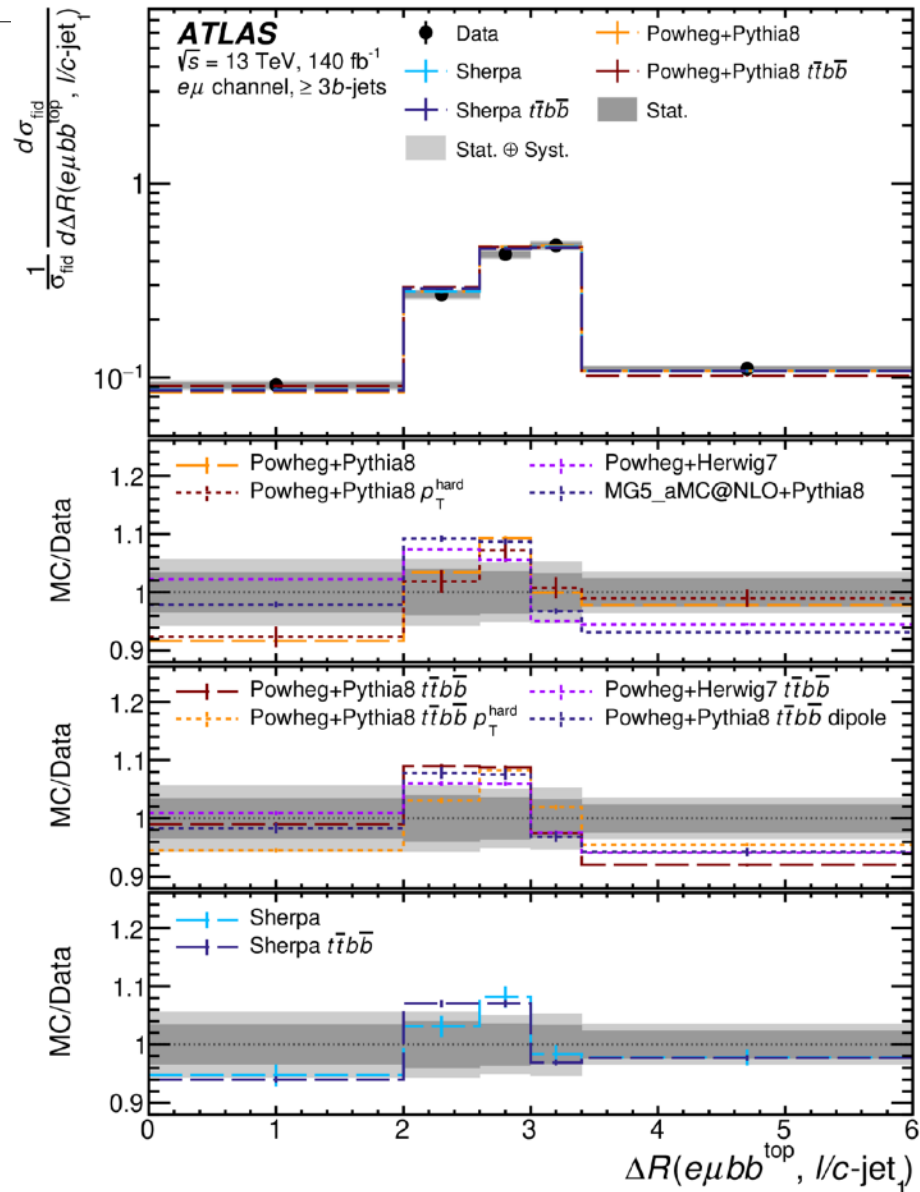
Phase-I L1 latest updates



Search for Long Lived Leptons



$t\bar{t}$ + b-jets association production cross-section



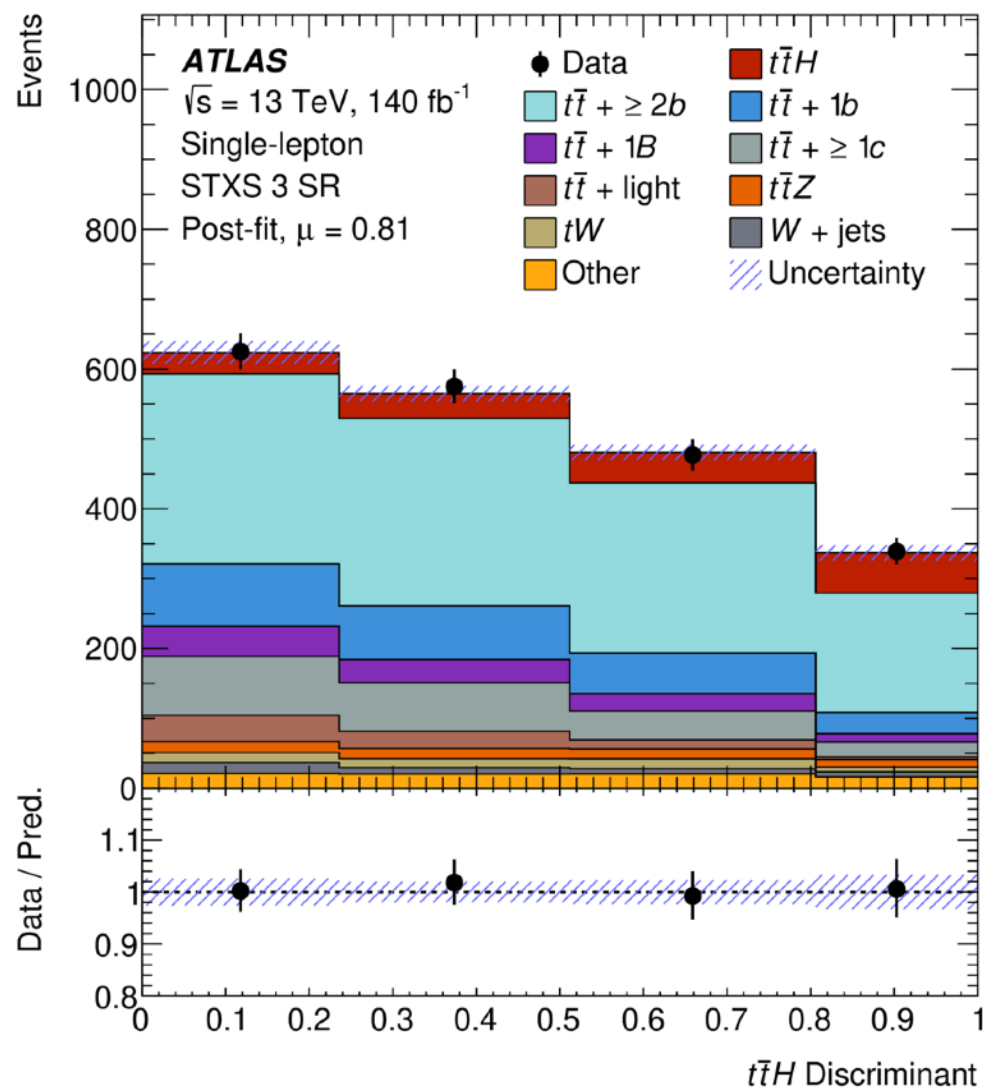
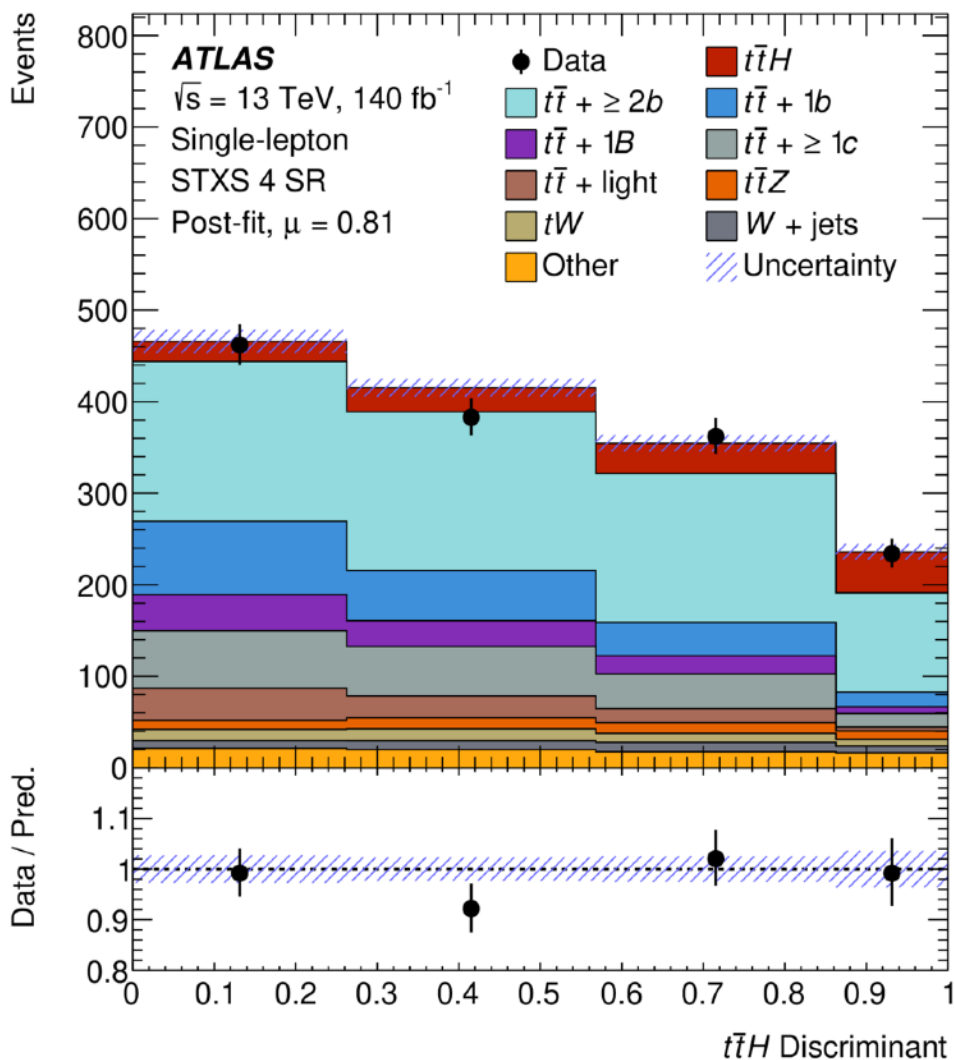
$t\bar{t}$ + b-jets association production cross-section



Observable	Description	Phase spaces				
		$\geq 2b$	$\geq 3b$	$\geq 3b$ $\geq 1l/c$	$\geq 4b$	$\geq 4b$ $\geq 1l/c$
σ^{fid}	Fiducial total cross-section		✓	✓	✓	✓
$N_{b\text{-jets}}$	Number of b -jets	✓	✓			
$N_{l/c\text{-jets}}$	Number of light- or c -jets		✓		✓	
H_T^{had}	Scalar sum of p_T of all jets		✓		✓	
H_T^{all}	Scalar sum of p_T of charged leptons, jet and missing E_T		✓		✓	
$\Delta R_{\text{avg}}^{bb}$	Average angular distance in ΔR of b -jet pairs		✓		✓	
$\Delta\eta_{\text{max}}^{jj}$	Maximum absolute difference in η between any pair of jets		✓		✓	
$p_T(b_1)$	p_T of the hardest b -jet		✓		✓	
$p_T(b_2)$	p_T of second-hardest b -jet		✓		✓	
$p_T(b_3)$	p_T of third-hardest b -jet		✓		✓	
$p_T(b_4)$	p_T of fourth-hardest b -jet				✓	
$\eta(b_1)$	η of hardest b -jet		✓		✓	
$\eta(b_2)$	η of second-hardest b -jet		✓		✓	
$\eta(b_3)$	η of third-hardest b -jet		✓		✓	
$\eta(b_4)$	η of fourth-hardest b -jet				✓	
$p_T(l/c\text{-jet}_1)$	p_T of the hardest light- or c -jet			✓		✓
$\eta(l/c\text{-jet}_1)$	η of the hardest light- or c -jet			✓		✓
$m(b_1b_2)$	Invariant mass of two hardest b -jets in p_T		✓		✓	
$\Delta R(b_1, b_2)$	ΔR between two hardest b -jets		✓		✓	
$p_T(b_1b_2)$	p_T of two hardest b -jets		✓		✓	
$m(bb^{\text{min}\Delta R})$	Invariant mass of two closest b -jets in ΔR				✓	
$p_T(bb^{\text{min}\Delta R})$	p_T of the closest b -jets pair				✓	
$\text{min}\Delta R(bb)$	Closest angular distance in ΔR among b -jets				✓	
$m(e\mu b_1b_2)$	Invariant mass of electron, muon and two hardest b -jets		✓		✓	
$p_T(b_1^{\text{top}})$	p_T of the hardest b -jet assigned to top quark		✓		✓	
$p_T(b_2^{\text{top}})$	p_T of the second-hardest b -jet assigned to top quark		✓		✓	
$p_T(b_1^{\text{add}})$	p_T of the hardest additional b -jet		✓		✓	
$p_T(b_2^{\text{add}})$	p_T of the second-hardest additional b -jet				✓	
$\eta(b_1^{\text{top}})$	η of the hardest b -jet assigned to top quark		✓		✓	
$\eta(b_2^{\text{top}})$	η of the second-hardest b -jet assigned to top quark		✓		✓	
$\eta(b_1^{\text{add}})$	η of the hardest additional b -jet		✓		✓	
$\eta(b_2^{\text{add}})$	η of the second-hardest additional b -jet				✓	
$m(b\bar{b}^{\text{top}})$	Invariant mass of a pair of b -jets assigned to top quarks		✓		✓	
$p_T(b\bar{b}^{\text{top}})$	p_T of a pair of b -jets assigned to top quarks		✓		✓	
$m(b\bar{b}^{\text{add}})$	Invariant mass of a pair of additional b -jets				✓	
$p_T(b\bar{b}^{\text{add}})$	p_T of a pair of additional b -jets				✓	
$m(e\mu b\bar{b}^{\text{top}})$	Invariant mass of $e\mu$ and the b -jets pair assigned to top quarks		✓		✓	
$\Delta R(e\mu b\bar{b}^{\text{top}}, b_1^{\text{add}})$	ΔR between the direction of the system of $e\mu$ and b -jet pair assigned to top and the direction of the hardest additional b -jet		✓		✓	
$\Delta R(e\mu b\bar{b}^{\text{top}}, l/c\text{-jet}_1)$	ΔR between the direction of the system of $e\mu$ and b -jet pair assigned to top and the direction of the hardest light- or c -jet			✓		✓
$p_T(l/c\text{-jet}_1) - p_T(b_1^{\text{add}})$	Difference in p_T between the hardest l/c -jet and the additional b -jet			✓		✓

Summary of all measured observables in each fiducial phase space region. The availability of an observable is indicated by checkmark in the last five columns. The first half of the table lists the global event variables and the kinematics of b -jets ordered in p_T , whereas the second half lists the quantities specific to the b -jets assigned to top quark decays or to extra $b\bar{b}$ system as well as those related to the additional light- or c -jets (l/c -jets).

Higgs coupling to heavy flavour, $t\bar{t}H(\rightarrow b\bar{b})$

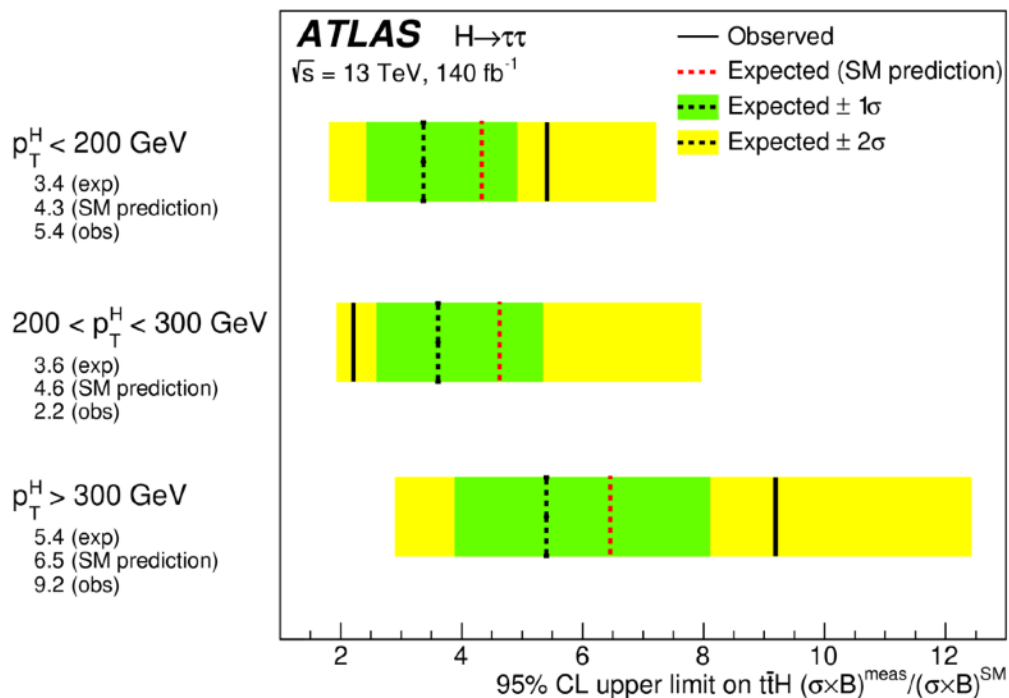


Higgs coupling to heavy flavour, $t\bar{t}H(\rightarrow b\bar{b})$

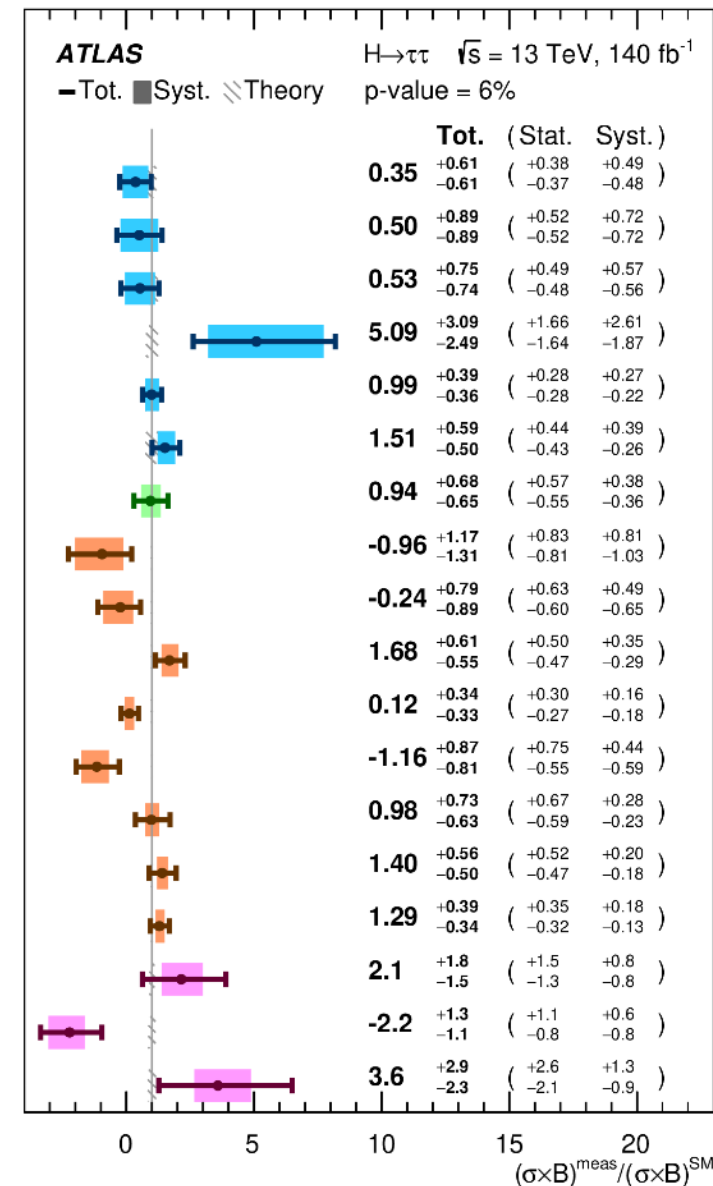
Uncertainty source	$\Delta\sigma_{t\bar{t}H}$ (fb)		$\Delta\sigma_{t\bar{t}H}/\sigma_{t\bar{t}H}$ (%)	
Process modelling				
$t\bar{t}H$ modelling				
$t\bar{t}H$ radiation	+35	-21	+9	-5
$t\bar{t}H$ parton shower	+32	-19	+8	-5
$t\bar{t}H$ matching	<0.1	-0.3	<0.1	-0.1
$t\bar{t}H$ theory	+25	-17	+6	-4
$t\bar{t} + \geq 1b$ modelling				
$t\bar{t} + \geq 1b$ radiation	± 31		± 8	
$t\bar{t} + \geq 1b$ parton shower	± 29		± 7	
$t\bar{t} + \geq 1b$ matching	± 19		± 5	
$t\bar{t} + \geq 1c$ modelling	± 18		± 4	
$t\bar{t} + \text{light}$ modelling	± 5		± 1	
tW modelling	± 16		± 4	
Minor background modelling	± 19		± 5	
Flavour tagging	± 36		± 9	
Jet modelling	± 22		± 5	
Monte-Carlo statistics	± 17		± 4	
Other instrumental	± 10		± 2	
Total systematic uncertainty	+85	-75	+21	-18
Normalisation factors	± 21		± 5	
Total statistical uncertainty	± 54		± 13	
Total uncertainty	+101	-92	+25	-22

A list of the absolute and relative uncertainties in the measured $\sigma_{t\bar{t}H}$ grouped in categories. The contributions from different sources of uncertainty are evaluated after the fit. The quoted values are obtained by repeating the fit, while fixing the set of nuisance parameters of the sources corresponding to each category to their best-fit values, and subtracting in quadrature the resulting uncertainty from the total uncertainty of the nominal fit presented in the last row. The total uncertainty is different from the sum in quadrature of the different components due to correlations between nuisance parameters in the fit. The $t\bar{t}H$ and $t\bar{t} + \geq 1b$ radiation uncertainty categories include the renormalisation and factorisation scales, ISR and FSR uncertainties. The " $t\bar{t}H$ theory" category includes STXS-related theoretical uncertainties and uncertainty in the $H \rightarrow b\bar{b}$ branching fraction. The "Minor background modelling" category includes uncertainties in the fake-lepton background and in minor backgrounds as defined in the text. The total statistical uncertainty includes uncertainties in the normalisation factors.

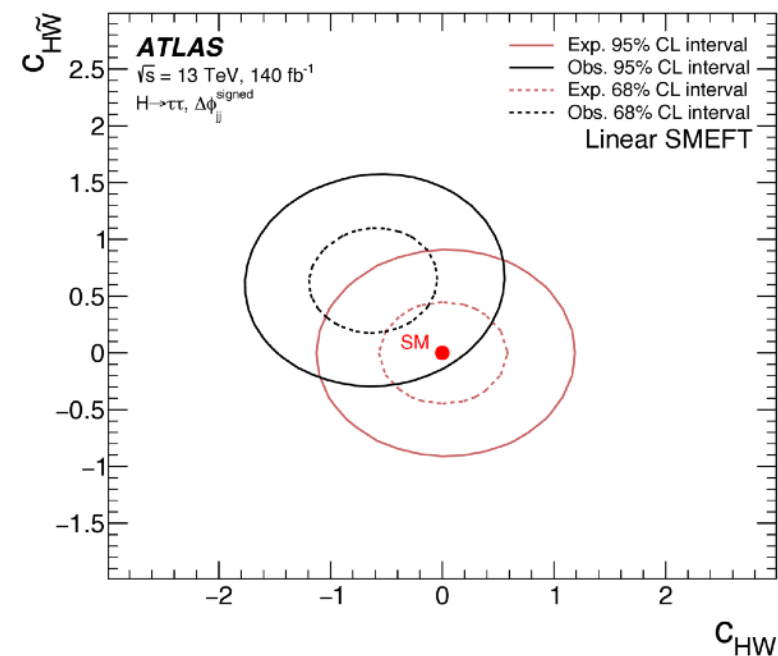
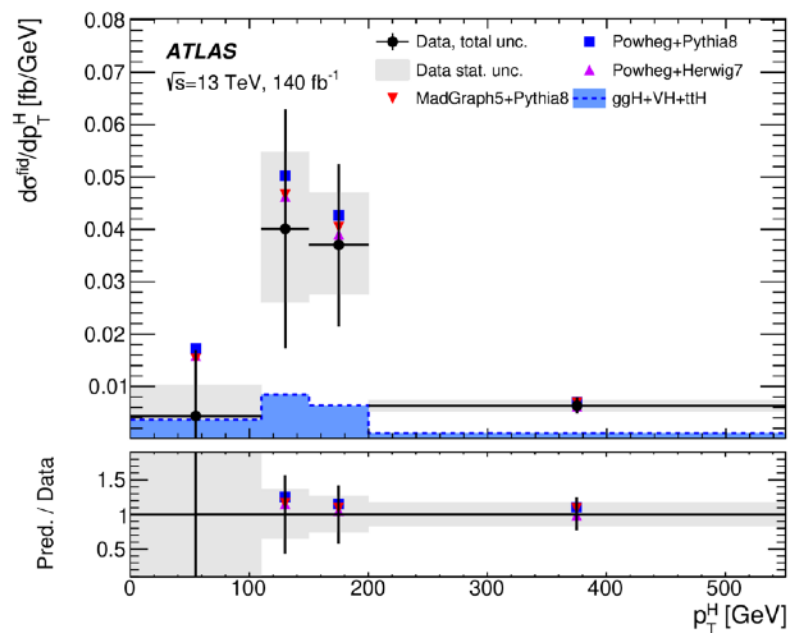
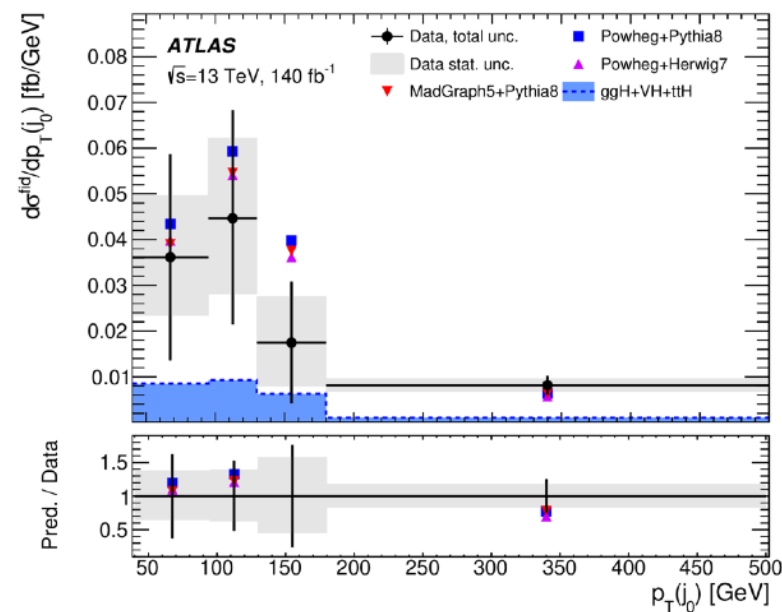
Higgs coupling to third lepton generation, $H \rightarrow \tau\tau$



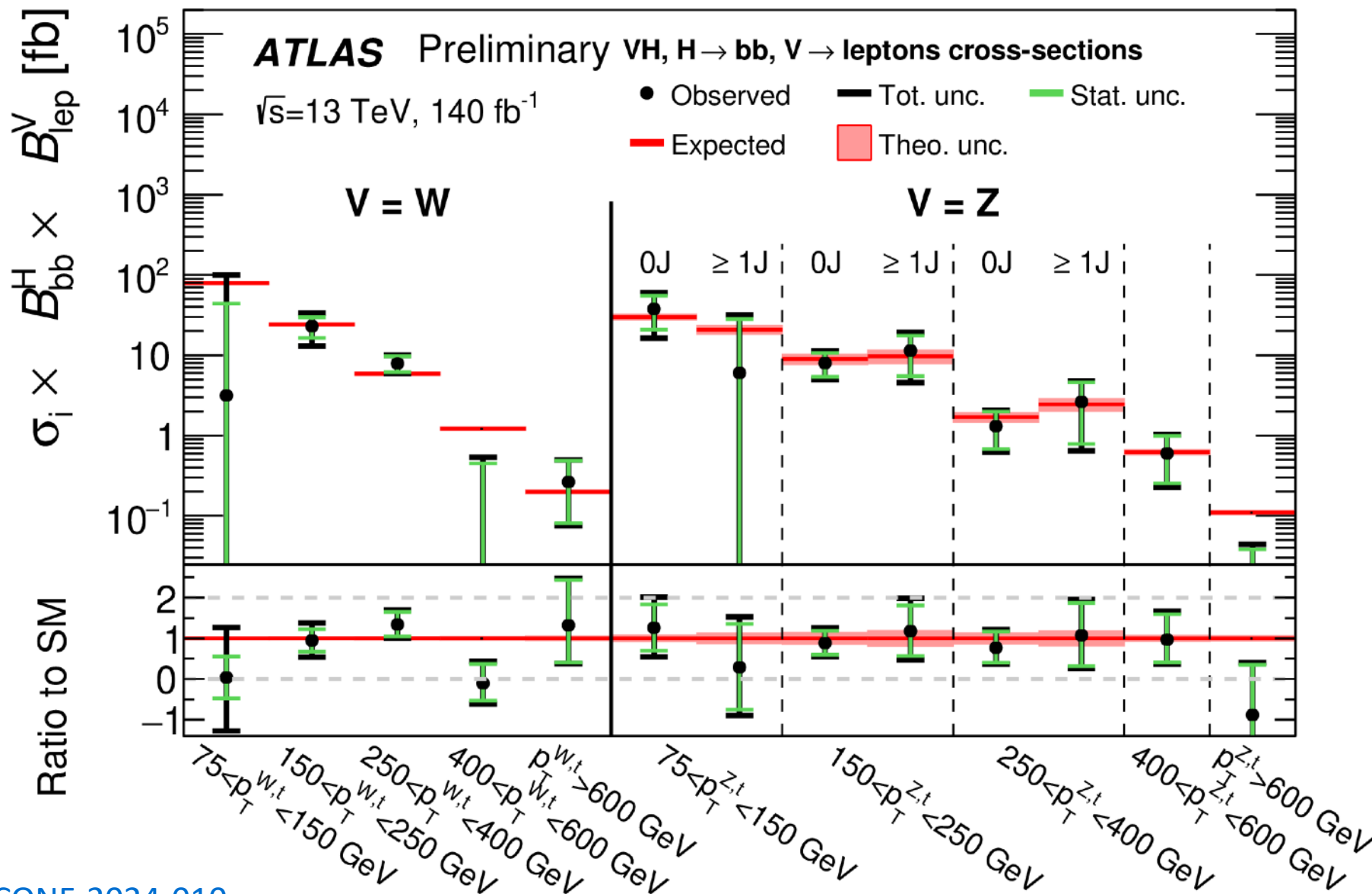
$gg \rightarrow H, 1\text{-jet}, 120 \leq p_T^H < 200 \text{ GeV}$	0.35	+0.61 -0.61	(+0.38 -0.37)	(+0.49 -0.48)
$gg \rightarrow H, \geq 1\text{-jet}, 60 \leq p_T^H < 120 \text{ GeV}$	0.50	+0.89 -0.89	(+0.52 -0.52)	(+0.72 -0.72)
$gg \rightarrow H, \geq 2\text{-jet}, m_{jj} < 350, 120 \leq p_T^H < 200 \text{ GeV}$	0.53	+0.75 -0.74	(+0.49 -0.48)	(+0.57 -0.56)
$gg \rightarrow H, \geq 2\text{-jet}, m_{jj} \geq 350 \text{ GeV}, p_T^H < 200 \text{ GeV}$	5.09	+3.09 -2.49	(+1.66 -1.64)	(+2.61 -1.87)
$gg \rightarrow H, 200 \leq p_T^H < 300 \text{ GeV}$	0.99	+0.39 -0.36	(+0.28 -0.28)	(+0.27 -0.22)
$gg \rightarrow H, p_T^H \geq 300 \text{ GeV}$	1.51	+0.59 -0.50	(+0.44 -0.43)	(+0.39 -0.26)
$qq' \rightarrow Hqq', \geq 2\text{-jet}, 60 \leq m_{jj} < 120 \text{ GeV}$	0.94	+0.68 -0.65	(+0.57 -0.55)	(+0.38 -0.36)
$qq' \rightarrow Hqq', \geq 2\text{-jet}, 350 \leq m_{jj} < 700 \text{ GeV}, p_T^H < 200 \text{ GeV}$	-0.96	+1.17 -1.31	(+0.83 -0.81)	(+0.81 -1.03)
$qq' \rightarrow Hqq', \geq 2\text{-jet}, 700 \leq m_{jj} < 1000 \text{ GeV}, p_T^H < 200 \text{ GeV}$	-0.24	+0.79 -0.89	(+0.63 -0.60)	(+0.49 -0.65)
$qq' \rightarrow Hqq', \geq 2\text{-jet}, 1000 \leq m_{jj} < 1500 \text{ GeV}, p_T^H < 200 \text{ GeV}$	1.68	+0.61 -0.55	(+0.50 -0.47)	(+0.35 -0.29)
$qq' \rightarrow Hqq', \geq 2\text{-jet}, m_{jj} \geq 1500 \text{ GeV}, p_T^H < 200 \text{ GeV}$	0.12	+0.34 -0.33	(+0.30 -0.27)	(+0.16 -0.18)
$qq' \rightarrow Hqq', \geq 2\text{-jet}, 350 \leq m_{jj} < 700 \text{ GeV}, p_T^H \geq 200 \text{ GeV}$	-1.16	+0.87 -0.81	(+0.75 -0.55)	(+0.44 -0.59)
$qq' \rightarrow Hqq', \geq 2\text{-jet}, 700 \leq m_{jj} < 1000 \text{ GeV}, p_T^H \geq 200 \text{ GeV}$	0.98	+0.73 -0.63	(+0.67 -0.59)	(+0.28 -0.23)
$qq' \rightarrow Hqq', \geq 2\text{-jet}, 1000 \leq m_{jj} < 1500 \text{ GeV}, p_T^H \geq 200 \text{ GeV}$	1.40	+0.56 -0.50	(+0.52 -0.47)	(+0.20 -0.18)
$qq' \rightarrow Hqq', \geq 2\text{-jet}, m_{jj} \geq 1500 \text{ GeV}, p_T^H \geq 200 \text{ GeV}$	1.29	+0.39 -0.34	(+0.35 -0.32)	(+0.18 -0.13)
$t\bar{t}H, p_T^H < 200 \text{ GeV}$	2.1	+1.8 -1.5	(+1.5 -1.3)	(+0.8 -0.8)
$t\bar{t}H, 200 \leq p_T^H < 300 \text{ GeV}$	-2.2	+1.3 -1.1	(+1.1 -0.8)	(+0.6 -0.8)
$t\bar{t}H, p_T^H \geq 300 \text{ GeV}$	3.6	+2.9 -2.3	(+2.6 -2.1)	(+1.3 -0.9)



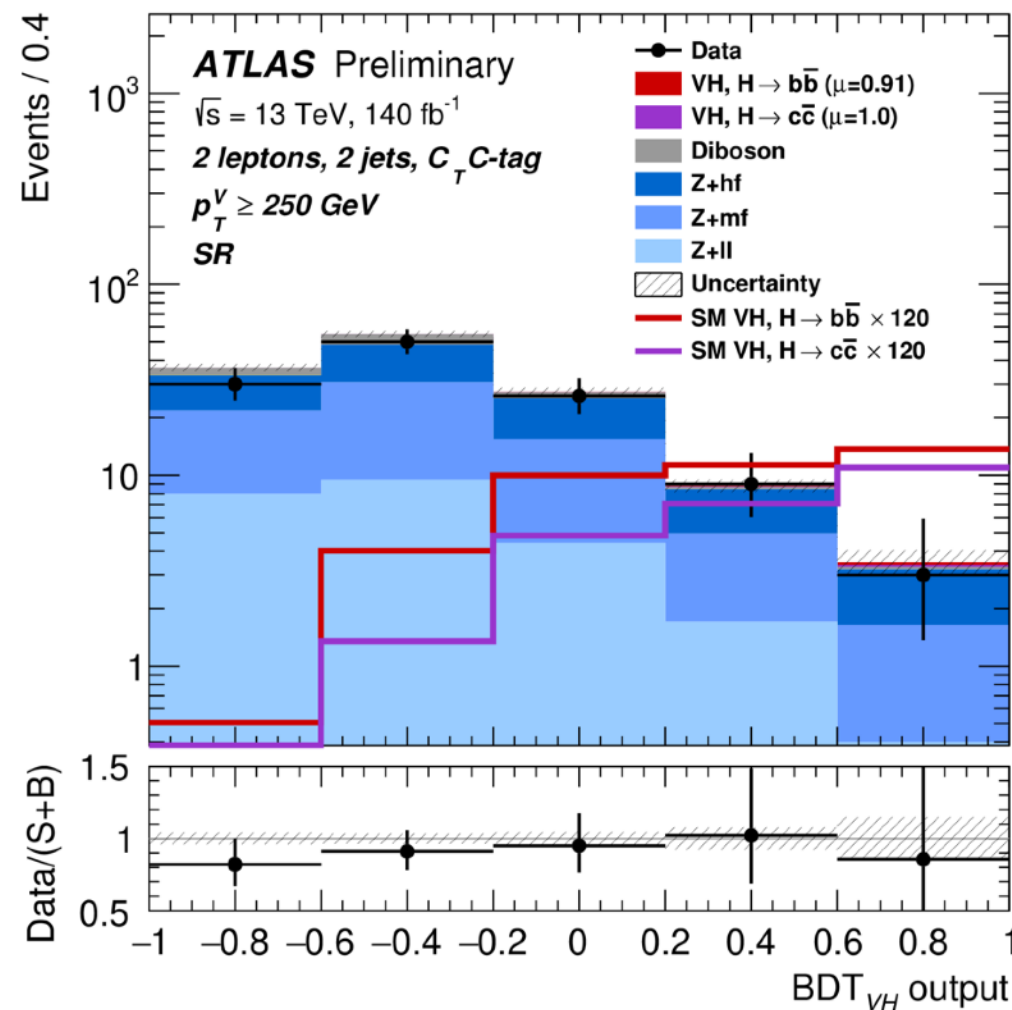
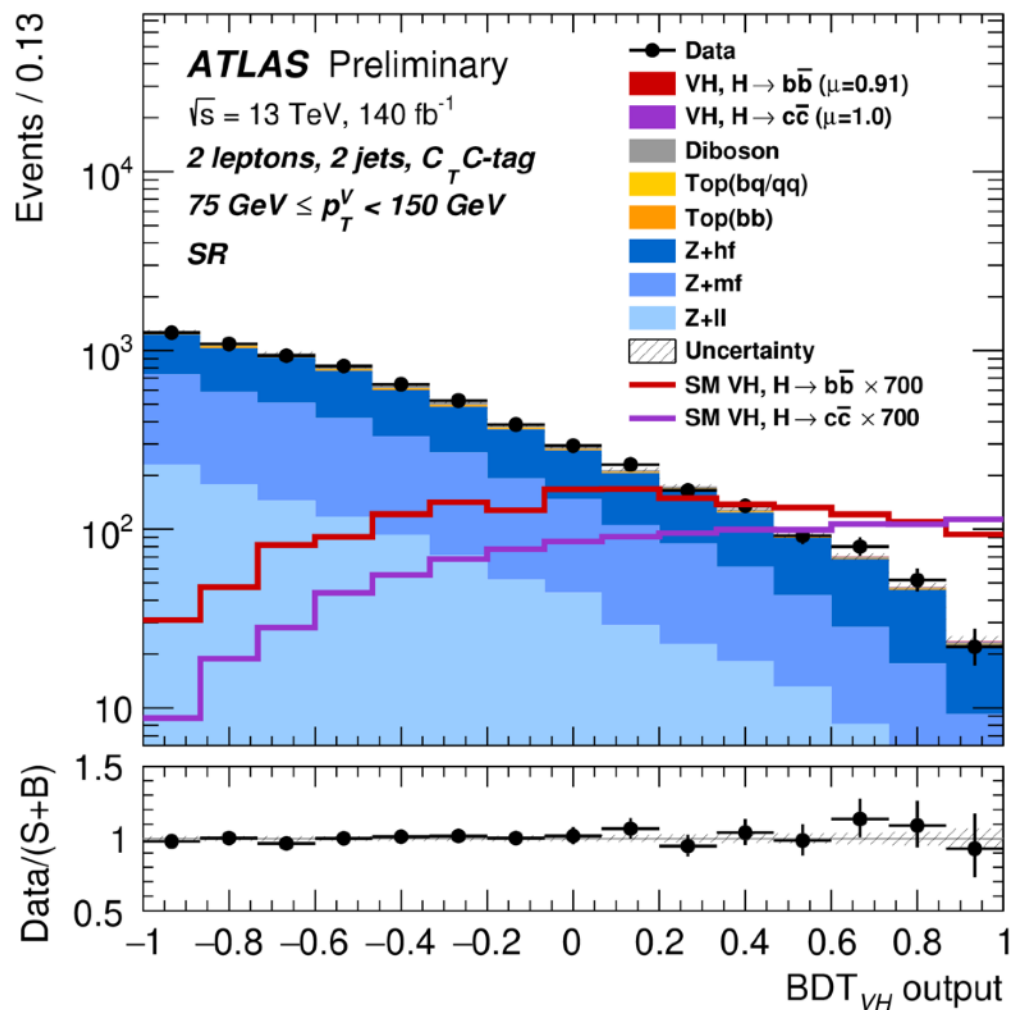
Higgs coupling to third lepton generation, $H \rightarrow \tau\tau$



Higgs coupling to second quark generation, $H \rightarrow c\bar{c}$



Higgs coupling to second quark generation, $H \rightarrow c\bar{c}$



Higgs coupling to second quark generation, $H \rightarrow c\bar{c}$

